1999

Critical adsorption on curved objects

Andreas Hanke
The University of Texas Rio Grande Valley

S. Dietrich

Recommended Citation

Hanke, A., and S. Dietrich. "Critical Adsorption on Curved Objects." Physical Review E, vol. 59, no. 5, American Physical Society, May 1999, pp. 5081–100, doi:10.1103/PhysRevE.59.5081.

Critical adsorption on curved objects

A. Hanke and S. Dietrich
Fachbereich Physik, Bergische Universität Wuppertal, D-42097 Wuppertal, Federal Republic of Germany
(Received 25 September 1998)

A systematic field-theoretical description of critical adsorption on curved objects such as spherical or rodlike colloidal particles immersed in a fluid near criticality is presented. The temperature dependence of the corresponding order parameter profiles and of the excess adsorption are calculated explicitly. Critical adsorption on elongated rods is substantially more pronounced than on spherical particles. It turns out that, within the context of critical phenomena in confined geometries, critical adsorption on a microscopically thin ''needle'' represents a distinct universality class of its own. Under favorable conditions the results are relevant for the flocculation of colloidal particles. [S1063-651X(99)10305-2]

PACS number(s): 64.60.Fr, 68.35.Rh, 82.70.Dd, 64.75.+g

I. INTRODUCTION

In colloidal suspensions the interaction between the mesoscopic dissolved particles and the solvent is of basic importance [1,2]. For example, the solvent generates effective interactions between the colloidal particles which can even lead to flocculation. The richness of the physical properties of these systems is mainly based on the possibility to tune these effective interactions over wide ranges of strength and form of the interaction potential. Traditionally this tuning is accomplished by changing the chemical composition of the solvent, e.g., by adding salt, polymers, or other components [1]. Compared with such modifications, changes of the temperature or pressure typically result only in minor changes of the effective interactions. This, however, is only true as long as the solvent is not thermodynamically close to a phase transition of its own. For example, if the solvent consists of a binary liquid mixture close to a *first-order* demixing transition into a *A*-rich and a *B*-rich liquid phase, even slight changes of the temperature or of the partial pressures of the two species *A* and *B* can lead to massive changes of the effective interactions between dissolved colloid particles induced by the occurrence of wetting transitions. They lead to wetting films of the preferred phase coating the colloidal particles [3]. These wetting films can snap into bridges if the particles come close to each other leading to flocculation [4,5]. For charged colloidal particles such as silica spheres immersed in the binary liquid mixture of water and 2,6-lutidine [4] flocculation can also be influenced by screening effects generated by the adsorbed layers [6].

Similarly drastic effects can occur if the solvent is brought close to a *critical point*. The inevitable preference of the surfaces of the colloidal particles for one of the two solvent species of a binary liquid mixture near its critical demixing point or for the liquid phase of a solvent fluid near its liquid-vapor critical point results into the presence of effective surface fields leading to pronounced adsorption profiles of the preferred component. This so-called ''critical adsorption'' becomes particularly long-ranged due to the correlation effects induced by the critical fluctuations of the order parameter of the solvent. In the case of a planar wall critical adsorption has been studied in much detail [7–16]. Asymptotically close to the critical point T_c its universal properties are linked to the *critical adsorption fixed point* of the corresponding renormalization group description. The ensuing scaling functions near the surface of a spherical particle with radius R refer to the simultaneous scaling limit $T \to T_c$, $s \to \infty$, and $R \to \infty$, where s is the distance from the confining surface. In this limit the ratio s/R is kept fixed forming a finite scaling variable. *At* the critical adsorption fixed point the surface field is infinitely large so that the order parameter profile diverges upon approaching the surface. We recall that such divergences refer to the renormalization group fixed point whereas actually the divergence of the order parameter profile is cut off at atomic distances σ from the surface.

As compared to a planar surface critical adsorption on a spherical particle is expected to exhibit important differences in behavior because the confining surface has a positive curvature and because a sphere represents only a quasi-zero-dimensional defect floating in the critical fluid. The interference of critical adsorption on neighboring spheres gives rise to the so-called critical Casimir forces [17] which have been argued to contribute to the occurrence of flocculation near T_c [18–20]. A quantitative understanding of these phenomena requires the knowledge of the critical adsorption profiles near the colloidal particles and the resulting effective free energy of interaction in the whole vicinity of the critical point, i.e., as functions of both the reduced temperature $t = (T - T_c)/T_c$ and the field h conjugate to the order parameter. This ambitious goal has not yet been accomplished. Instead, the introduction of a surface curvature has limited the knowledge of the corresponding critical adsorption so far to the case of spheres for the particular thermodynamic state $(t,h) = (0,0)$ of the solvent [21,22]. Only recently at least the temperature dependence of the critical Casimir force between a sphere and a planar container wall has been addressed [23]. Thus the present study of the temperature dependence of critical adsorption on a single sphere contributes one step towards reaching the aforementioned general goal.

Apart from spherical particles, also rodlike particles play an important role [24]. Rodlike objects are provided, e.g., by fibers or colloidal rods [24], semiflexible polymers with a large persistence length such as actin [25], microtubuli [25], and carbon nanotubes [26]. Moreover the knowledge of the general curvature dependence of critical adsorption is also relevant, e.g., for curved membranes [27,28] dissolved in a fluid near criticality or for the liquid-vapor interface between

a binary liquid mixture near its critical demixing point and its noncritical vapor, which exhibits rippled configurations due to the occurrence of capillary waves [27].

Near criticality the relevant length scales of the solvent structures are dominated by the diverging bulk correlation length $\xi_{\pm}=\xi_0^{\pm}|t|^{-\nu}$, where ν is the standard universal bulk critical exponent; ξ_0^{+} and ξ_0^{-} are nonuniversal amplitudes in the one- $(+)$ and two-phase region $(-)$, respectively, with values typically in the order of a few Å. In practice the correlation length can span the range between 5 Å -1 μm depending on t. In the present context this length scale is played off against the length scale R of the radius of the dissolved particles. We note that the available systems can realize both the limit $R/\xi \gg 1$ as well as the opposite limit $R/\xi \ll 1$. In the case of Ludox silica particles $R \approx 12$ nm [29] so that the limit $R/\xi \ll 1$ can be easily achieved even with the upper limits for ξ set by finite experimental resolutions. The ratio of the length l and the radius R of rodlike particles can be quite large, in conjunction with a small radius such as $R \approx 7$ nm in the case of colloidal boehmite rods [24]. In this work we consider *long* rods, i.e., $R,\xi \ll l$, and neglect effects which may arise due to their finite length l.

In the present contribution we investigate systematically the temperature dependence of the critical adsorption on a single spherical or rodlike particle, i.e., the case $(t \neq 0, h=0)$. (The generalization to the case $h \neq 0$ is straightforward but tedious.) In order to be able to treat spheres and cylinders in a unified way within a field-theoretical approach and for general spatial dimensions D it is helpful to consider the particle shape of a *generalized cylinder* K [30] with an infinitely extended ''axis'' of dimension δ. The ''axis'' can be the axis of an ordinary infinitely elongated cylinder $(\delta=1)$, or the midplane of a slab $(\delta=D-1)$, or the center of a sphere $(\delta=0)$. For general integer D and δ the explicit form of K is

$$K=\{\mathbf{r}=(\mathbf{r}_{\perp},\mathbf{r}_{\parallel}) \in \mathbb{R}^{D-\delta}\times\mathbb{R}^{\delta};\ |\mathbf{r}_{\perp}| \leqslant R\} \tag{1.1}$$

with $\mathbf{r}_{\perp}$ and $\mathbf{r}_{\parallel}$ perpendicular and parallel to the axis, respectively (see Fig. 1). Note that $\mathbf{r}_{\perp}$ is a d-dimensional vector with

$$d=D-\delta. \tag{1.2}$$

The radius R of the generalized cylinder K is the radius in the cases of an ordinary cylinder or a sphere and it is half of the thickness in the case of a slab. For the slab the geometry reduces to the much studied case of (two decoupled) half spaces. The generalization of D to values different from three is introduced for technical reasons because $D_{\mathrm{uc}}=4$ marks the upper critical dimension for the relevance of fluctuations of the order parameter leading to a behavior different from that obtained from mean-field theory valid for $D=4$.

In Sec. II we discuss the general scaling properties of the local order parameter profiles for critical adsorption on spheres and cylinders, in particular the behavior close to the particle surfaces and for small particle radii, respectively. In Sec. III we consider the corresponding properties of the excess adsorption. In Sec. IV we present explicit results both for the order parameter profiles and for the excess adsorption in mean-field approximation. Section V contains our conclusions. In Appendix A we discuss the two-point correlation function near a microscopically thin ''needle'' at criticality. In Appendix B we determine a universal amplitude and a universal scaling function as needed in Secs. II and III, respectively. In Appendix C, finally, we consider the general curvature dependence of the excess adsorption.

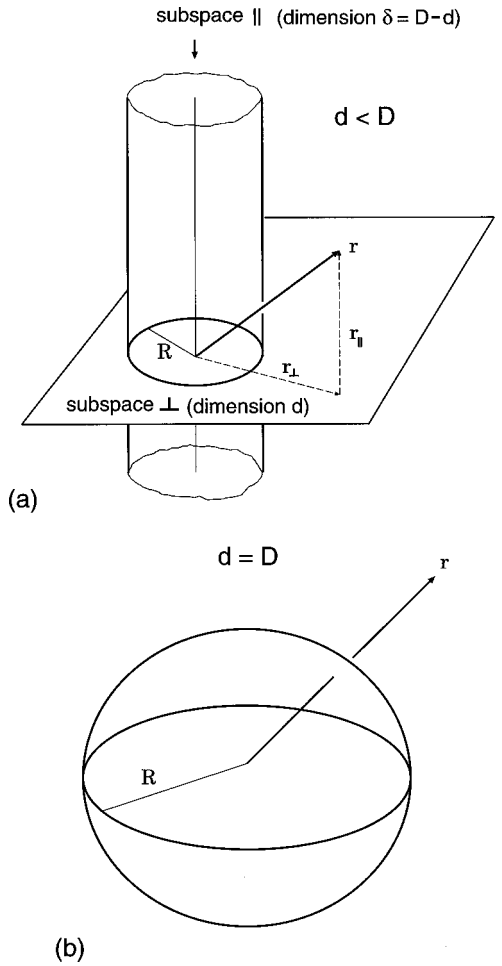

FIG. 1. (a) A generalized cylinder K with $d<D$ [i.e., $\delta=D-d>0$, see Eq. (1.1)] and (b) a sphere as the special case of K with $d=D$ as examples of particles with curved boundaries. D is the spatial dimension. The point $\mathbf{r}=(\mathbf{r}_{\perp},\mathbf{r}_{\parallel})$ at which, e.g., the order parameter is monitored is also shown.

II. ORDER PARAMETER PROFILES

A. General scaling properties

Asymptotically close to T_c (compare the second paragraph of the Introduction) critical adsorption on the surface of a sphere or cylinder with radius R is characterized by an order parameter profile $\langle\Phi(\mathbf{r})\rangle_t$ which for $h=0$ takes the scaling form

$$\langle\Phi(\mathbf{r})\rangle_t = a|t|^{\beta}P_{\pm}(s/\xi_{\pm},R/\xi_{\pm}) \tag{2.1}$$

for radial distances $s=r_{\perp}-R \gtrsim \sigma$ from the surface larger than a typical microscopic length σ. Here $\langle\ \rangle_t$ denotes the thermal average in the presence of a sphere or a cylinder and β is the standard universal bulk critical exponent. The scaling functions $P_{\pm}$ depend on two scaling variables

$$x_\pm = s/\xi_\pm\,, \quad y_\pm = R/\xi_\pm\,. \tag{2.2}$$

The scaling functions $P_\pm$ are *universal* while the nonuniversal *bulk* amplitudes a and $\xi_0^\pm$ are determined by the value $\langle\Phi\rangle_{t,\,b} = a|t|^\beta$ for $t<0$, $t\to 0^-$ of the order parameter in the unbounded bulk and by the amplitudes of the correlation length, respectively. (In this work we are always concerned with the Ising universality class.) We note that the form of $P_\pm$ depends on the definition used for the correlation length $\xi_\pm$. For definiteness we adopt $\xi_\pm$ as being the *true* correlation length fixed by the exponential decay of the two-point correlation function in real space [31]. Bearing this in mind one finds that $P_{+,\,b} \equiv P_+(\infty, y_+) = 0$, $P_{-,\,b} \equiv P_-(\infty, y_-) = 1$, and $P_\pm(x_\pm \to \infty, y_\pm) - P_{\pm,\,b} \sim \exp(-x_\pm)$ where the prefactor in front of the exponential may by an algebraic function of $x_\pm$ (see Sec. IV).

On the other hand, in the limit $y_\pm \to \infty$ with $x_\pm$ fixed the scaling functions $P_\pm(x_\pm, y_\pm)$ reduce to

$$P_\pm(x_\pm) \equiv P_\pm(x_\pm, \infty), \quad \text{half-space}, \tag{2.3}$$

corresponding to the half-space bounded by a planar surface. In recent years the scaling functions $P_\pm(x_\pm)$ for the half-space have been intensively studied theoretically [9,12–14] and compared with experiments [9,14–16]. For later reference we quote some of their properties. First, we note the asymptotic behavior [12]

$$P_\pm(x_\pm \to 0) \to c_\pm\, x_\pm^{-\beta/\nu} \times [1 + \overline{a}_\pm\, x_\pm^{1/\nu} + \overline{a}'_\pm\, x_\pm^{2/\nu} + \overline{b}_\pm\, x_\pm^{D} + \cdots] \tag{2.4}$$

with universal amplitudes $c_\pm$, $\overline{a}_\pm$, $\overline{a}'_\pm$, and $\overline{b}_\pm$ [32] which depend, however, on the definition of the correlation length [31]. The ellipses stand for contributions which vanish more rapidly than $x_\pm^D$. The exponent β/ν is the bulk ''scaling dimension'' [33] of the order parameter Φ. For convenience of the reader we quote their numerical values [33,9]

$$\beta(D=4) = 1/2, \quad \beta(3) \simeq 0.328, \quad \beta(2) = 1/8, \tag{2.5a}$$

$$\nu(D=4) = 1/2, \quad \nu(3) \simeq 0.632, \quad \nu(2) = 1, \tag{2.5b}$$

so that

$$(\beta/\nu)\,(4) = 1, \quad (\beta/\nu)\,(3) \simeq 0.519, \quad (\beta/\nu)\,(2) = 1/8. \tag{2.5c}$$

The leading power law in Eq. (2.4) is a consequence of the fact that due to the presence of the symmetry breaking surface field the limit $t\to 0$ must lead to a nonvanishing order parameter profile at $t=0$ so that

$$\langle\Phi(\mathbf{r})\rangle_{\mathrm{hs},\,t=0} = a\, c_\pm\, (s/\xi_0^\pm)^{-\beta/\nu}. \tag{2.6}$$

(The subscript hs stands for half-space.) Thus the amplitude of the power law $s^{-\beta/\nu}$ in Eq. (2.6) consists of the combination $a\,(\xi_0^\pm)^{\beta/\nu}$ of nonuniversal bulk amplitudes and of the universal surface amplitude $c_\pm$. Because the left-hand side (LHS) of Eq. (2.6) does not depend on how the limit $t=0$ is approached, the universal amplitudes c_+ and c_- are related via the universal bulk ratio ξ_0^+/ξ_0^-:

$$\frac{c_-}{c_+} = \left(\frac{\xi_0^+}{\xi_0^-}\right)^{\beta/\nu}. \tag{2.7}$$

The terms proportional to $\overline{a}_\pm$ and $\overline{a}'_\pm$ in Eq. (2.4) correspond to *regular* contributions for $t\to 0$ of the order parameter since

$$\langle\Phi(\mathbf{r})\rangle_{\mathrm{hs},\,t} \overset{t\to 0}{\to} \langle\Phi(\mathbf{r})\rangle_{\mathrm{hs},\,t=0} \times [1 + A\,t + A'\,t^2 + B_\pm |t|^{2-\alpha} + \cdots], \tag{2.8}$$

where $A = \pm\,\overline{a}_\pm (s/\xi_0^\pm)^{1/\nu}$ and $A' = \overline{a}'_\pm (s/\xi_0^\pm)^{2/\nu}$ are *independent* of the sign of t [12]. The term proportional to $\overline{b}_\pm$ in Eq. (2.4) corresponds to the first singular contribution [34] for $t\to 0$ of the order parameter leading to the term $B_\pm |t|^{2-\alpha}$ in Eq. (2.8) with the bulk exponent $\alpha = 2 - \nu D$ and $B_\pm = \overline{b}_\pm (s/\xi_0^\pm)^D$.

Figure 2 summarizes theoretical results for $P_\pm(x_\pm)$ for the spatial dimensions $D=4$, 3, and 2. In $D=4$ the functions $P_\pm$ are given by the following mean-field expressions:

$$P_+(x_+) = \frac{\sqrt{2}}{\sinh(x_+)}, \quad P_-(x_-) = \coth\left(\frac{x_-}{2}\right), \quad D=4. \tag{2.9}$$

The results for $D=3$ represent recent Monte Carlo (MC) simulations [13,15] and field-theoretical renormalization group (RG) calculations [12,15]. For $D=2$ exact results are available from the semi-infinite two-dimensional Ising model [35]. Note that $P_\pm(x_\pm)$ for any fixed value of $x_\pm$ *decreases* with decreasing D [36]. This reflects the general trend that critical fluctuations, which reduce the mean value of the order parameter, are more pronounced in lower spatial dimensions.

The curves in the inset of Fig. 2 are scaled so that they demonstrate the leading behavior of $P_\pm(x_\pm \to 0)$. (A similar representation will be used in Sec. IV.) In Table I we quote the corresponding numerical values of the surface amplitudes $c_\pm$ and $\overline{a}_\pm$ according to Eq. (2.4). In order to achieve a presentation in the inset of Fig. 2(b) which reflects both the leading behavior of $P_-(x_- \to 0)$ and the exponential decay $P_-(x_- \to \infty) - 1 \sim \exp(-x_-)$ we introduce the function

$$U(x_-) = \tanh\left(\frac{x_-^2}{x_- + 1}\right). \tag{2.10}$$

The curves in the inset of Fig. 2(b) comply with the above condition since $U(x_- \to 0) \sim x_-^2$ and $U(x_- \to \infty) - 1 \sim \exp(-2x_-)$ so that in both limits the leading asymptotic behaviors of $P_-(x_-)$ are not changed.

In the remaining part of this section we discuss the new features of $P_\pm(x_\pm, y_\pm)$ which arise for $y_\pm < \infty$. First, we consider the short distance behavior for $s\to 0$, which corresponds to the limit $x_\pm \to 0$ with $y_\pm$ fixed. Then, we consider cases in which the radius R is small compared with $\xi_\pm$ as

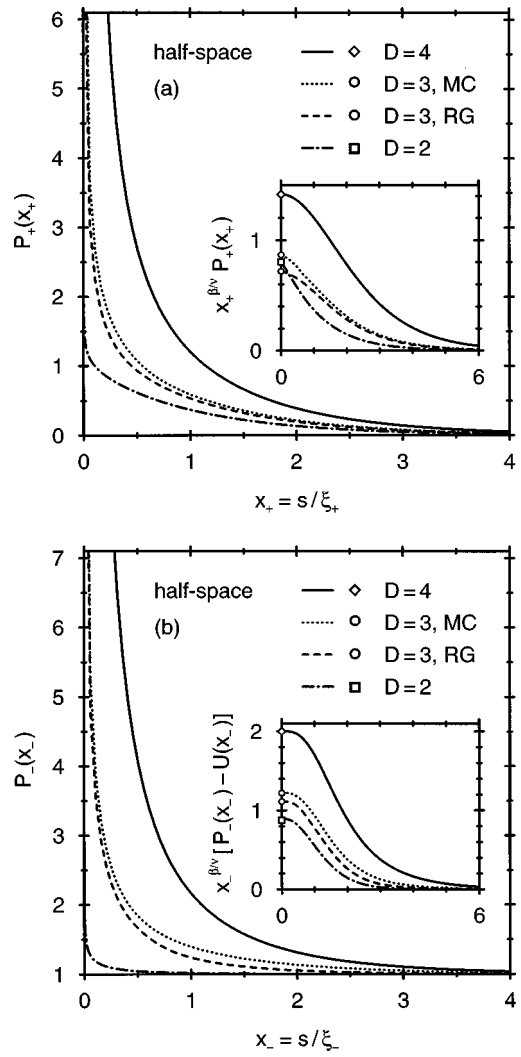

FIG. 2. (a) Universal scaling function $P_+(x_+)$ for critical adsorption on a planar surface in spatial dimensions $D=4$, 3, and 2. The estimates for $P_+(x_+)$ in $D=3$ labeled MC and RG are obtained by Monte Carlo simulations and field-theoretical renormalization-group calculations. We display the corresponding data presented in Ref. [15]. The inset shows a scaled version of $P_+(x_+)$ which reflects, in particular, the asymptotic behavior of $P_+(x_+\to 0)$. The open symbols indicate the corresponding values of c_+ [see Eq. (2.4) and Table I]. (b) Same representation as in (a) for the universal scaling function $P_-(x_-)$. The inset shows a scaled version of $P_-(x_-)$ which contains the function $U(x_-)$ defined in Eq. (2.10) in order to facilitate a similar representation as in the inset of (a).

well as the distance between the sphere or the cylinder and the point for which the order parameter is monitored. This corresponds to the limit $y_\pm \to 0$ with $x_\pm$ fixed. It turns out that in this limit the behaviors for a sphere and a cylinder in $D=3$ are *qualitatively* different.

B. Short distance expansion

The same reasoning leading to Eq. (2.6) in case of the half-space yields for the generalized cylinder

$$\langle \Phi(\mathbf{r})\rangle_{t=0} = a\, \mathcal{C}_\pm(\Delta)\, (s/\xi_0^\pm)^{-\beta/\nu}, \quad \Delta = s/R, \tag{2.11}$$

i.e., the universal amplitude $c_\pm$ in Eq. (2.6) is generalized to the universal amplitude *function* $\mathcal{C}_\pm(\Delta)$. This function appears in the asymptotic behavior

$$P_\pm\left(x_\pm, y_\pm = \frac{x_\pm}{\Delta}\right) \to \mathcal{C}_\pm(\Delta)\ x_\pm^{-\beta/\nu}, \quad x_\pm \to 0, \quad \Delta \text{ fixed}, \tag{2.12}$$

which underscores that $\mathcal{C}_\pm(\Delta)$ is universal but depends on the definition of the correlation length [31] [compare Eq. (2.4)] and on the geometry. Since the limit $\Delta \to 0$ must reproduce the behavior for the half-space one has $\mathcal{C}_\pm(0) = c_\pm$. According to Eq. (2.7) the functions $\mathcal{C}_+(\Delta)$ and $\mathcal{C}_-(\Delta)$ are proportional to each other with

$$\frac{\mathcal{C}_-(\Delta)}{\mathcal{C}_+(\Delta)} = \frac{c_-}{c_+} = \left(\frac{\xi_0^+}{\xi_0^-}\right)^{\beta/\nu}. \tag{2.13}$$

Therefore it is sufficient to study only one of these functions, say, $\mathcal{C}_+(\Delta)$, which according to Eqs. (2.11) and (2.6) can be written as

$$\mathcal{C}_+(\Delta) = c_+ \langle \Phi(\mathbf{r})\rangle_{t=0} / \langle \Phi(\mathbf{r})\rangle_{\mathrm{hs},\, t=0}. \tag{2.14}$$

In the case of a sphere, i.e., $d=D$, the universal scaling function $\mathcal{C}_+(\Delta)$ is known exactly for any spatial dimension D of interest by means of a finite conformal mapping from the half-space [21]. It takes the simple analytic form

$$\mathcal{C}_+(\Delta) = c_+ \left(1 + \frac{\Delta}{2}\right)^{-\beta/\nu}, \quad d=D, \tag{2.15}$$

and depends on D only via the corresponding values of c_+ and β/ν. For large distances from the sphere, i.e., $\Delta \gg 1$, the function $\mathcal{C}_+(\Delta)$ in Eq. (2.15) decays as $\Delta^{-\beta/\nu}$ (compare the

TABLE I. Numerical values of the universal amplitudes $c_\pm$ and $\overline{a}_\pm$ [see Eq. (2.4)].

D	c_+	c_-	$\overline{a}_+$	$\overline{a}_-$
4	$\sqrt{2} \simeq 1.414$	2	$-\frac{1}{6} \simeq -0.167$	$\frac{1}{12} \simeq 0.083$
3, MC [a]	0.866	1.22		
3, RG [b]	0.717	1.113	-0.389	0.129
3, interpolation [c]	0.94 ± 0.05	1.24 ± 0.05		
2	0.803	0.876	$-\frac{1}{2} = -0.5$	$\frac{1}{4} = 0.25$

[a]Reference [15].

[b]Reference [15]; for $\overline{a}_\pm$ we use in addition Eq. (48) in Ref. [12] for $\varepsilon = 1$.

[c]Reference [14]; obtained from interpolating between the results in $D=4-\varepsilon$ and $D=2$.

following subsection). In the opposite limit $\Delta \to 0$, which is of interest in the present subsection, one has

$$\frac{\mathcal{C}_+(\Delta \to 0)}{c_+} = 1 - \frac{\beta/\nu}{2}\Delta + \frac{\beta/\nu\,(\beta/\nu+1)}{8}\Delta^2 + \mathcal{O}(\Delta^3), \qquad d = D. \tag{2.16}$$

We note, first, that an expansion such as in Eq. (2.16) is expected to hold not only near the surface of a sphere but also near a smoothly curved surface of *more general shape*. According to differential geometry up to second order in curvature the short distance expansion near a $(D-1)$-dimensional surface of arbitrary shape involves only the geometric invariants K_m, K_m^2, and K_G with [37,38]

$$K_m = \frac{1}{2}\sum_{i=1}^{D-1}\frac{1}{R_i} \tag{2.17a}$$

and

$$K_G = \sum_{\substack{\text{pairs}\\ i<j}}^{D-1}\frac{1}{R_i R_j}, \tag{2.17b}$$

where R_i are the $D-1$ principal local radii of curvature. In $D=3$ Eq. (2.17) yields the familiar expressions for the local mean curvature and the local Gaussian curvature. Second, we note that Eq. (2.16) reflects a property of the fluctuating order parameter field $\Phi(\mathbf{r})$ (or ''operator'') in the outer space of the sphere itself. In this spirit also near a surface of more general shape the short distance expansion can be formulated in ''operator form:''

$$\Phi(\mathbf{r})/\langle\Phi(\mathbf{r})\rangle_{\mathrm{hs},\,t=0} = [\mathbf{1}]\{1 + \kappa_1 K_m s + \kappa_2 K_m^2 s^2 + \kappa_G K_G s^2 + \mathcal{O}(s^3)\} + \mathcal{O}(s^D). \tag{2.18}$$

Here s is the distance of $\mathbf{r}$ to the nearest point of the surface. The terms on the right-hand side (RHS) of Eq. (2.18) should be interpreted as operators which are located *at* this point of the surface, i.e., as *surface operators*. On the RHS of Eq. (2.18) only such terms are shown explicitly which are proportional to the unity operator $[\mathbf{1}]$. The corrections emerge from curvatures of higher order and surface operators of different types which are expected to scale with powers of s at least of the order s^D [compare Eq. (2.4) for the half-space and Ref. [34]]. Thus for $D>2$ the terms displayed in Eq. (2.18) represent the leading contributions of the short distance expansion of $\Phi(\mathbf{r})$. The dimensionless coefficients κ_1, κ_2, and κ_G depend on D but not on the shape of the boundary surface. Comparison of Eq. (2.18) with Eq. (2.16) for the sphere, or direct calculation near a surface of arbitrary shape [10], yields

$$\kappa_1 = -\frac{\beta/\nu}{D-1}. \tag{2.19}$$

In $D=3$ the coefficients κ_2 and κ_G in Eq. (2.18) cannot be determined by comparison with Eq. (2.16) for the sphere alone. To this end one would need, in addition, the knowledge of the expansion for at least one curved surface of different shape (e.g., the surface of a cylinder). However, since in $D=3$ the sphere has the property $K_G = K_m^2$ the comparison of Eq. (2.18) with Eq. (2.16) determines at least the sum

$$\kappa_2 + \kappa_G = \frac{\beta/\nu\,(\beta/\nu+1)}{8}, \quad D=3. \tag{2.20}$$

In Sec. IV we confirm Eq. (2.18) and determine κ_1, κ_2, and κ_G for $D=4$.

The expansion (2.18) holds upon inserting it into thermal averages if the distance s to the curved surface—albeit being large on the microscopic scale—is much smaller than other characteristic length scales such as the correlation length or the distances to the remaining operators in correlation functions. For certain thermal averages such as the profile $\langle\Phi(\mathbf{r})\rangle_t$ additional *regular* terms can occur on the RHS [compare Eq. (2.8) for the half-space]. For spheres and cylinders, in particular, the expansion (2.18) determines the leading contributions to the scaling functions $P_\pm(x_\pm, y_\pm)$ generated by the surface curvature. For the surface of a generalized cylinder the curvatures in Eq. (2.17) are given by

$$K_m = \frac{d-1}{2}\frac{1}{R} \tag{2.21a}$$

and

$$K_G = \frac{(d-1)(d-2)}{2}\frac{1}{R^2}. \tag{2.21b}$$

By inserting these expressions into Eq. (2.18) and using Eq. (2.1) one obtains

$$P_\pm(x_\pm \to 0, y_\pm)\big|_{\mathrm{sde}} \to c_\pm\, x_\pm^{-\beta/\nu}\left\{1 + \kappa_1\frac{d-1}{2}\Delta + \left[\kappa_2\frac{(d-1)^2}{4} + \kappa_G\frac{(d-1)(d-2)}{2}\right]\Delta^2 + \mathcal{O}(\Delta^3)\right\} \tag{2.22}$$

for $x_\pm \to 0$ with $y_\pm$ fixed so that $\Delta = x_\pm/y_\pm \to 0$ [the subscript sde refers to the short distance operator expansion in Eq. (2.18)].

Note that Eq. (2.22) does not contain the abovementioned regular contributions. Upon employing Eq. (2.4) for the half-space, however, one can obtain the asymptotic expansion of $P_\pm(x_\pm \to 0, y_\pm)$ including the leading regular term. Assuming that for $t \gtrless 0$ the profile $\langle\Phi(\mathbf{r})\rangle_t$ is still analytic in $1/R$ one finds

$$P_\pm(x_\pm \to 0, y_\pm) \to c_\pm\, x_\pm^{-\beta/\nu}\left\{1 + \kappa_1\frac{d-1}{2}\Delta + \left[\kappa_2\frac{(d-1)^2}{4} + \kappa_G\frac{(d-1)(d-2)}{2}\right]\Delta^2 + \overline{a}_\pm\, x_\pm^{1/\nu} + \cdots\right\} \tag{2.23}$$

for $x_\pm \to 0$ with $y_\pm$ fixed so that $\Delta = x_\pm / y_\pm \to 0$. The ellipses stand for contributions which vanish more rapidly than $x_\pm^2$ if $D>2$ [39]. The universal amplitudes $c_\pm$ and $\bar{a}_\pm$ are the same as in Eq. (2.4) (see Table I) and κ_1, κ_2, and κ_G are from Eqs. (2.19) and (2.20). In Sec. IV we shall confirm Eq. (2.23) explicitly for $D=4$.

C. Spheres and cylinders with small radii

In this subsection we consider spheres and cylinders whose radii are much smaller than other characteristic lengths such as the correlation length or the distance between the particle and the point at which the order parameter is monitored. In these limiting cases the effect of the particle upon the fluctuating order parameter distribution can be represented by a δ-function potential located at the center of the particle which enhances the value of the order parameter. It is instructive to consider this expansion for the generalized cylinder K for which this δ-function potential is smeared out over its axis, i.e., the Boltzmann weight $\exp(-\delta\mathcal{H}_K)$ of K, where $\delta\mathcal{H}_K$ is the difference of the Hamiltonian describing the system with and without the presence of K (whose axis includes the origin), can be systematically expanded in a series with increasing powers of R [19,23], i.e.,

$$\exp(-\delta\mathcal{H}_K) \propto 1 + \mathcal{E}_{d,D} R^{\beta/\nu - D + d} w_K + \cdots, \quad (2.24)$$

where $\mathcal{E}_{d,D}$ is an amplitude and

$$w_K = \begin{cases} \int_{\mathbb{R}^\delta} d^{\,\delta} r_\parallel \;\; \Phi(\mathbf{r}_\perp = 0, \mathbf{r}_\parallel), & d < D, \\ \Phi(0), & d = D. \end{cases} \quad (2.25)$$

Here only the leading nontrivial contribution for $R \to 0$ is shown explicitly and the ellipses stand for contributions which vanish more rapidly for $R \to 0$. For the case that K is a *sphere* [19], i.e., $d=D$, the amplitude $\mathcal{E}_{D,D}$ is equal to the ratio $A_\uparrow^\Phi / B_\Phi$, where $A_\uparrow^\Phi$ and B_Φ are amplitudes of the half-space profile

$$\langle \Phi(\mathbf{r}) \rangle_{\mathrm{hs},\, t=0} = A_\uparrow^\Phi (2s)^{-\beta/\nu} \quad (2.26)$$

at the critical point of the fluid for the boundary condition $\uparrow$ corresponding to the critical adsorption fixed point and of the bulk two-point correlation function

$$\langle \Phi(\mathbf{r}) \Phi(0) \rangle_{b,\, t=0} = B_\Phi\, r^{-2\beta/\nu} \quad (2.27)$$

at criticality, respectively. The ratio $(A_\uparrow^\Phi)^2 / B_\Phi$ is universal [23]. The comparison of Eq. (2.26) with Eq. (2.6) yields the relation

$$A_\uparrow^\Phi = a\, (2\xi_0^\pm)^{\beta/\nu}\, c_\pm \quad (2.28)$$

between the nonuniversal amplitudes $A_\uparrow^\Phi$, a, $\xi_0^\pm$, and the universal amplitude $c_\pm$.

It is crucial to observe that Eq. (2.24) is only valid if the exponent of R is *positive*, i.e.,

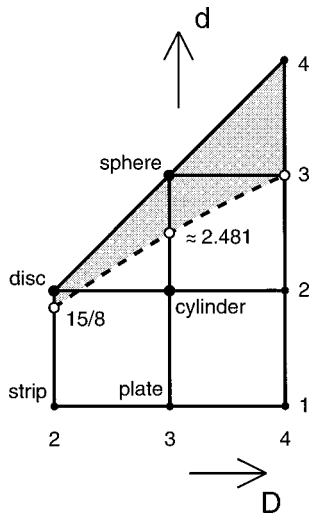

FIG. 3. Diagram of generalized cylinders K which behave—in the renormalization group sense—as relevant or irrelevant perturbations of a fluid near criticality. The parameter $d \leqslant D$ characterizes the shape of K and D is the space dimension [see Eq. (1.1)]. The point $(d,D)=(2,2)$ corresponds to a disc in $D=2$ and the points (3,3) and (2,3) to a sphere and an infinitely elongated cylinder in $D=3$, respectively. The line with $D=4$ and arbitrary d represents the upper critical dimension for which the mean-field results for the adsorption profiles are exact (see Sec. IV). The open circles indicate points (d,D) for which $d=D-(\beta/\nu)(D)$ within the Ising universality class. These points are connected by the dashed line so that within the shaded region *above* it the small radius expansion (2.24) is valid [see Eq. (2.29)] and K represents an irrelevant perturbation. Points (d,D) below the broken line, such as the cylinder in $D=3$, are characterized by the fact that the order parameter at large distances from K deviates from its bulk value even if the radius R is microscopically small, which means that K represents a relevant perturbation.

$$\beta/\nu - D + d > 0. \quad (2.29)$$

Figure 3 shows as a dashed line $d=D-(\beta/\nu)(D)$ [40] in the (d,D) plane which separates generalized cylinders K which are *relevant* perturbations for the fluctuating order parameter field (such as the strip in $D=2$ or the plate in $D=3$) from those which are *irrelevant* and for which Eq. (2.24) applies. Thus, the disc in $D=2$ and the sphere in $D=3$ represent irrelevant perturbations whereas the cylinder in $D=3$ represents a relevant perturbation. This implies that an infinitely elongated cylinder in $D=3$ generates a perturbation of the order parameter from its bulk value whose spatial extension is only limited by the bulk correlation length. The order parameter profile becomes even independent of R in the formal limit $R \to 0$, i.e., if the cylinder radius R becomes microscopically small [41]. The critical adsorption transition on such a microscopically thin ''needle'' is characterized by critical exponents which need not be equal to the corresponding exponents for the bulk or the half-space (see Appendix A). For the disc in $D=2$ and the sphere in $D=3$, in contrast, the deviation of the order parameter from its bulk value vanishes in the limit $R \to 0$. This is reflected by Eq. (2.24) which is—apart from the condition in Eq. (2.29)—only valid if the small radius R is still large on the microscopic scale.

The line $d=D-(\beta/\nu)(D)$ itself corresponds to marginal perturbations leading to a behavior which in general is dif-

ferent from Eq. (2.24). We shall neither discuss this nor the crossover from marginal behavior to the behavior described by Eq. (2.24) which may arise for points closely above the line. The line $d=D-(\beta/\nu)(D)$ includes, in particular, the generalized cylinder with $d=3$ and $D=4$ (see Sec. IV). The marginal behavior of this particular generalized cylinder, however, is not typical for spheres or cylinders in $D=3$, which are strictly irrelevant or relevant perturbations, respectively. Therefore in the following we shall generally speak of spheres if $d=D$ and speak of cylinders if $d=2$ and $D\geqslant 3$ (see Fig. 3).

We now turn to the consequences of Eq. (2.24) and the related properties of the universal scaling functions $\mathcal{C}_+(\Delta)$ and $P_\pm(x_\pm,y_\pm)$ defined in Eqs. (2.14) and (2.1). First, we consider the sphere, i.e., $d=D$, for which Eq. (2.24) applies. In order to obtain the asymptotic behavior of $\mathcal{C}_+(\Delta)$ for $\Delta=s/R\to\infty$ one basically replaces $\langle\Phi(\mathbf{r})\rangle_{t=0}$ in the numerator on the RHS of Eq. (2.14) by the *bulk* two-point correlation function $\langle\Phi(\mathbf{r})\Phi(0)\rangle_{b,\,t=0}$ where r can be replaced by s in leading order. By using Eqs. (2.26) and (2.27) in conjunction with $\mathcal{E}_{D,D}=A_\uparrow^\Phi/B_\Phi$ one finds

$$\mathcal{C}_+(\Delta\to\infty)\to c_+\left(\frac{\Delta}{2}\right)^{-\beta/\nu},\quad d=D. \tag{2.30}$$

This checks with the exact result for $\mathcal{C}_+(\Delta)$ in Eq. (2.15). For $t\gtrless 0$ and $y_\pm=R/\xi_\pm\to 0$ with $x_\pm=s/\xi_\pm>0$ fixed the same steps as above lead to

$$P_\pm(x_\pm,y_\pm\to 0)-P_{\pm,\,b}\to c_\pm(2y_\pm)^{\beta/\nu}x_\pm^{-2\beta/\nu}\mathcal{F}_\pm(x_\pm),\qquad d=D. \tag{2.31}$$

Here $\mathcal{F}_\pm$ is the *bulk* universal scaling function defined by (compare Appendix B)

$$\langle\Phi(\mathbf{r})\Phi(0)\rangle_{b,\,t}^{C}=B_\Phi\, r^{-2\beta/\nu}\mathcal{F}_\pm(r/\xi_\pm), \tag{2.32}$$

where the superscript C denotes the cumulant of the correlation function. Equations (2.32) and (2.27) imply the normalization $\mathcal{F}_\pm(0)=1$. According to the definition of $\xi_\pm$ as the true correlation length [compare the discussion below Eq. (2.2)] one has $\mathcal{F}_\pm(x_\pm\to\infty)\sim\exp(-x_\pm)$. Equation (2.31) implies that $P_\pm(x_\pm,y_\pm\to 0)$ decays to its bulk value with the power law $\sim y_\pm^{\beta/\nu}$ for *any* value of $x_\pm$.

Next, we consider the cylinder, i.e., $d=2$ and $D\geqslant 3$. In accordance with the discussion above this object represents a relevant perturbation. The order parameter deviates from its bulk value even for $R\to 0$ so that the universal scaling functions $\mathcal{C}_+(\Delta)$ and $P_\pm(x_\pm,y_\pm)$ remain finite in the limit $\Delta=s/R\to\infty$ and $y_\pm=R/\xi_\pm\to 0$, respectively. For $t=0$ this implies

$$\mathcal{C}_\pm(\Delta\to\infty)\to n_\pm,\quad d=2,D\geqslant 3, \tag{2.33}$$

which defines new universal amplitudes $n_\pm$ with $n_-/n_+=(\xi_0^+/\xi_0^-)^{\beta/\nu}$. Equations (2.33) and (2.11) imply that for $t=0$ the order parameter profile near a thin ''needle'' at distances s from the needle large compared with microscopic lengths takes the form

$$\langle\Phi(\mathbf{r})\rangle_{t=0}=a\,n_+(s/\xi_0^+)^{-\beta/\nu},\quad \text{needle}. \tag{2.34}$$

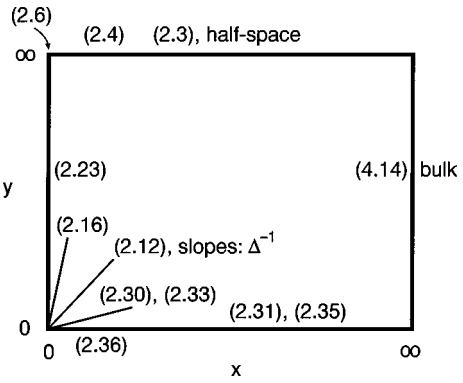

FIG. 4. The scaling functions $P_\pm(x_\pm=s/\xi_\pm,y_\pm=R/\xi_\pm)$ exhibit distinct behaviors for various limits of the variables $x_\pm$ and $y_\pm$. The position of an equation number in the (x,y) plane indicates the corresponding limiting case to which it applies. The case $y_\pm=\infty$ corresponds to the half-space [see Eq. (2.4) and Table I]. The short distance behavior for $s\to 0$ corresponds to the limit $x_\pm\to 0$ with $y_\pm$ fixed [see Eq. (2.23)]. The functions $\mathcal{C}_\pm(\Delta=s/R)$ in Eq. (2.12) characterize the behavior for $\xi_\pm\to\infty$, i.e., the limit $x_\pm\to 0$ with fixed ''slope'' $\Delta^{-1}=y_\pm/x_\pm$. The behavior for small R corresponds to the limit $y_\pm\to 0$ with $x_\pm$ fixed [see Eqs. (2.31) and (2.35)].

For $t\gtrless 0$ one finds

$$P_\pm(x_\pm,y_\pm\to 0)\to P_\pm(x_\pm,0)\equiv N_\pm(x_\pm),\quad d=2,D\geqslant 3, \tag{2.35}$$

where the new universal scaling functions $N_\pm(x_\pm)$ characterize the critical adsorption profile on a thin needle. In the limit $x_\pm\to 0$ they behave as

$$N_\pm(x_\pm\to 0)\to n_\pm x_\pm^{-\beta/\nu},\quad \text{needle}, \tag{2.36}$$

with $n_\pm$ from Eq. (2.33) [compare Eq. (2.4) for the half-space]. In Sec. IV we shall confirm Eqs. (2.33)–(2.36) and calculate $n_\pm$ and $N_\pm(x_\pm)$ explicitly for $D=4$. Figure 4 summarizes the various types of limiting behavior of the scaling functions $P_\pm(x_\pm,y_\pm)$.

III. EXCESS ADSORPTION

A. General scaling properties

Close to T_c the total enrichment of the preferred component of the fluid near the surface of the generalized cylinder is proportional to the excess adsorption $\Gamma(t,R)$ defined as

$$\Gamma(t,R)=\int_V d^Dr\,[\langle\Phi(\mathbf{r})\rangle_t-\langle\Phi\rangle_{t,\,b}]$$
$$=l^\delta\,\Omega_d\int_0^\infty ds\,(s+R)^{d-1}\,[\langle\Phi(\mathbf{r})\rangle_t-\langle\Phi\rangle_{t,\,b}]. \tag{3.1}$$

Here $V=\mathbb{R}^D\backslash K$ is the volume accessible to the critical fluid, i.e., the total space except for the volume occupied by the sphere or the cylinder K, and $\Omega_d=2\pi^{d/2}/\Gamma(d/2)$ is the surface area of the d-dimensional unit sphere. For a sphere one has $\delta=D-d=0$ and $l^\delta=1$ whereas for a cylinder $d=2$ so that in $D=3$ the quantity $l^\delta=l$ is the length of the cylinder.

In order to obtain the scaling behavior of $\Gamma(t,R)$ we split the s integration into the intervals $0 \leqslant s \leqslant \sigma$ and $s > \sigma$ where σ represents a typical microscopic length [14]. For the second interval one can use Eq. (2.1) which leads to

$$\Gamma(t,R) = l^{\delta}\Omega_d [I(t;\sigma,R) + J_{\pm}(y_{\pm};\sigma/\xi_{\pm})] \tag{3.2}$$

with

$$I(t;\sigma,R) = \int_0^{\sigma} ds\, (s+R)^{d-1} [\langle \Phi(\mathbf{r})\rangle_t - \langle \Phi \rangle_{t,b}], \tag{3.3}$$

$$J_{\pm}(y_{\pm};\sigma/\xi_{\pm}) = a\,|t|^{\beta}\,\xi_{\pm}^{d} \int_{\sigma/\xi_{\pm}}^{\infty} dx_{\pm}\,(x_{\pm}+y_{\pm})^{d-1} \times [P_{\pm}(x_{\pm},y_{\pm}) - P_{\pm,b}]. \tag{3.4}$$

In the limit $t \to 0$ the integral in Eq. (3.3) remains finite and yields a nonuniversal constant which is subdominant to the diverging contribution $J_{\pm}$ in Eq. (3.4). In order to clarify the dependence of the latter on $y_{\pm} = R/\xi_{\pm}$ we decompose it according to

$$J_{\pm}(y_{\pm};\sigma/\xi_{\pm}) = R^{d-1}\, a\, \xi_0^{\pm}\, |t|^{\beta-\nu} \left\{ \int_{\sigma/\xi_{\pm}}^{\infty} dx_{\pm} \times [P_{\pm}(x_{\pm}) - P_{\pm,b}] + G_{\pm}(y_{\pm};\sigma/\xi_{\pm}) \right\}, \tag{3.5}$$

where $P_{\pm}(x_{\pm}) = P_{\pm}(x_{\pm},\infty)$ are the scaling functions for the half-space and

$$G_{\pm}(y_{\pm};\sigma/\xi_{\pm}) = \int_{\sigma/\xi_{\pm}}^{\infty} dx_{\pm} \left\{ \left(\frac{x_{\pm}}{y_{\pm}} + 1 \right)^{d-1} [P_{\pm}(x_{\pm},y_{\pm}) - P_{\pm,b}] - [P_{\pm}(x_{\pm}) - P_{\pm,b}] \right\}. \tag{3.6a}$$

The comparison of Eq. (3.5) with Eq. (3.2) shows that the first term in curly brackets in Eq. (3.5) renders a contribution of the interval $s > \sigma$ to the excess adsorption per unit area as if the surface of the particle would be *planar* times the area $A = l^{\delta}\Omega_d R^{d-1}$ of the actually curved surface of a sphere or a cylinder. Thus the functions $G_{\pm}$ in Eq. (3.5) reflect the deviation of the excess adsorption on a curved surface from that on a planar surface beyond pure geometry.

In order to reveal the behavior of $J_{\pm}(y_{\pm};\sigma/\xi_{\pm})$ for $t \to 0$ it is necessary to study the integrals in Eqs. (3.5) and (3.6a) at their lower bounds $\sigma/\xi_{\pm} \to 0$. The integral in Eq. (3.5) can be analyzed along the lines of Sec. IIA in Ref. [14]. One finds that for $D < 4$ its contribution to $\Gamma(t \to 0,R)$ leads to the power law singularity $\sim |t|^{\beta-\nu}/(\nu-\beta)$ corresponding to a planar surface. The proper limit $D \nearrow 4$, for which $\nu \to \beta$ [see Eq. (2.5)], is accomplished by the presence of a term constant with respect to t which also diverges for $D \nearrow 4$ such that the sum leads to a contribution to $\Gamma(t \to 0,R)$ which diverges logarithmically in $D = 4$. The integral in Eq. (3.6a), however, remains finite for $\sigma/\xi_{\pm} \to 0$ also in $D = 4$ since the singular behavior for $x_{\pm} \to 0$ of the first term in curly brackets is cancelled by the second term. This implies that the function

$$G_{\pm}(y_{\pm}) \equiv G_{\pm}(y_{\pm};\, \sigma/\xi_{\pm} = 0) \tag{3.6b}$$

does indeed represent the leading behavior for $t \to 0$. Note that $G_{\pm}(y_{\pm})$ is universal because it depends only on the universal scaling functions $P_{\pm}(x_{\pm},y_{\pm})$ and $P_{\pm}(x_{\pm})$. In sum one finds

$$\Gamma(t \to 0,R) \to A\, a\, \xi_0^{\pm} \left\{ g_{\pm} \frac{|t|^{\beta-\nu}-1}{\nu-\beta} + |t|^{\beta-\nu} G_{\pm}(y_{\pm}) \right\}, \quad D \leqslant 4, \tag{3.7}$$

with the universal numbers (see Table II)

$$g_{\pm} = \begin{cases} (\nu-\beta) \displaystyle\int_0^{\infty} dx_{\pm} [P_{\pm}(x_{\pm}) - P_{\pm,b}], & D < 4, \\ \nu\, c_{\pm}, & D = 4, \end{cases} \tag{3.8}$$

where the second line is the limit for $D \nearrow 4$ of the first line. According to the above discussion one has $G_{\pm}(\infty) = 0$. Equation (3.7) generalizes the corresponding Eq. (2.10) in Ref. [14] for a planar surface by the additional second term in Eq. (3.7). A quantity accessible to experiments is the ratio

$$\mathcal{R}_{\Phi}(|t|,R) = \frac{\Gamma(+|t|,R)}{\Gamma(-|t|,R)} \tag{3.9a}$$

of the excess adsorptions above and below the critical point. The leading behavior of $\mathcal{R}_{\Phi}$ for $|t| \to 0$ is characterized by a universal function $R_{\Phi}(|t|,y_+,y_-)$, i.e.,

$$\mathcal{R}_{\Phi}(|t| \to 0,R) \to R_{\Phi}(|t|,y_+,y_-), \tag{3.9b}$$

which can be read off from Eqs. (3.9a) and (3.7). For a planar surface this function reduces to the universal number [14]

$$R_{\Phi} = \frac{\xi_0^+}{\xi_0^-}\frac{g_+}{g_-}, \quad \text{half-space.} \tag{3.10}$$

Table II summarizes theoretical results for $g_{\pm}$ and R_{Φ} corresponding to the half-space. For the curved surface of a sphere or cylinder, however, we shall see that for $y_{\pm} = R/\xi_{\pm} \to 0$ the divergence of the second term in curly

TABLE II. Numerical values of the universal numbers $g_{\pm}$ and R_{Φ} [see Eqs. (3.8) and (3.10)].

D	g_+	g_-	R_{Φ}
4	$\sqrt{2}/2 \simeq 0.707$	1	1
3, MC [a]	0.663	0.599	
3, RG [a]	0.581	0.438	
3, interpolation [b]	0.69 ± 0.1	0.56 ± 0.1	2.28 ± 0.1
2	0.910	0.0818	22.236

[a] Reference [15].
[b] Reference [14]; compare Table I.

brackets in Eq. (3.7) is more pronounced than the divergence of the first term. In order to clarify this aspect we now discuss the behavior of $G_\pm(y_\pm)$ in the limit for large and small values of $y_\pm$, respectively.

B. The scaling function $G_\pm(y_\pm)$ for $y_\pm \to \infty$

For $y_\pm \gg 1$ we assume that $G_\pm(y_\pm)$ is analytic in $y_\pm^{-1} = \xi_\pm / R$ so that it can be expanded into a Taylor series around $y_\pm^{-1} = 0$, i.e.,

$$G_\pm(y_\pm \to \infty) = a_{d,D}^\pm y_\pm^{-1} + b_{d,D}^\pm y_\pm^{-2} + \cdots \qquad (3.11)$$

[recall $G_\pm(\infty) = 0$ by definition]. The coefficients $a_{d,D}^\pm$ and $b_{d,D}^\pm$ are dimensionless and universal and depend on the space dimension D and on the shape of the generalized cylinder, i.e., on d. The validity of the expansion (3.11) is plausible since in the limit $\xi_\pm / R \ll 1$ the thickness $\sim \xi_\pm$ of the adsorbed layer is much smaller than the particle radius R so that a small curvature expansion should be applicable to $\Gamma(t \to 0, R)$ in Eq. (3.7) in which a surface term $\sim l^\delta R^{d-1}$ is followed by successive terms $\sim R^{d-2}$, R^{d-3}, etc., generated by the surface curvature. The terms on the RHS of Eq. (3.11) correspond to the leading curvature contributions to this expansion and imply that for decreasing values of $y_\pm = R/\xi_\pm \sim |t|^\nu$ the leading corrections to the first term in curly brackets in Eq. (3.7)—corresponding to a flat surface—are of the order $|t|^{\beta-\nu}|t|^{-n\nu}$ with $n = 1,2$, etc., and start to dominate it as soon as $y_\pm \lesssim 1$.

Similar as for the short distance expansion of the order parameter [compare Eq. (2.18)] the first Taylor coefficients of the expansion of $G_\pm(y_\pm \to \infty)$ also determine the curvature parameters of a particle $\mathcal{K}$ of *more general shape* provided its surface S is smooth and all principal radii of curvature are much larger than $\xi_\pm$. In this case one expects an expansion of the general form

$$\Gamma(t \to 0, R) = a\, \xi_0^\pm \int_S dS \left\{ g_\pm \frac{|t|^{\beta-\nu} - 1}{\nu - \beta} + \lambda_1^\pm K_m + \lambda_2^\pm K_m^2 + \lambda_G^\pm K_G + \cdots \right\}, \qquad (3.12)$$

where the curvatures K_m and K_G are given for a $(D-1)$-dimensional surface of general shape in Eq. (2.17). For the special case that the particle $\mathcal{K}$ is a generalized cylinder K the curvatures K_m and K_G are given by Eq. (2.21) and the comparison of Eq. (3.12) with Eqs. (3.7) and (3.11) yields

$$\lambda_1^\pm \frac{d-1}{2} = |t|^{\beta-\nu} a_{d,D}^\pm \xi_\pm \qquad (3.13a)$$

and the relation

$$\lambda_2^\pm \frac{(d-1)^2}{4} + \lambda_G^\pm \frac{(d-1)(d-2)}{2} = |t|^{\beta-\nu} b_{d,D}^\pm \xi_\pm^2 . \qquad (3.13b)$$

The curvature parameters $\lambda_1^\pm$, $\lambda_2^\pm$, and $\lambda_G^\pm$ depend on D but should not depend on the shape of K, i.e., on d in Eq. (3.13). This implies a corresponding dependence on d of $a_{d,D}^\pm$ and $b_{d,D}^\pm$, which provides an important consistency check for the validity of Eq. (3.12). In Sec. IV we confirm this dependence and explicitly calculate the curvature parameters for $D = 4$.

C. The scaling function $G_\pm(y_\pm)$ for $y_\pm \to 0$

In order to investigate this limit it is convenient to consider the function

$$y_\pm^{d-1} G_\pm(y_\pm) = \int_0^\infty dx_\pm \{ (x_\pm + y_\pm)^{d-1} [P_\pm(x_\pm, y_\pm) - P_{\pm,b}] - y_\pm^{d-1} [P_\pm(x_\pm) - P_{\pm,b}] \}. \qquad (3.14)$$

Because for $y_\pm \to 0$ the function $P_\pm(x_\pm, y_\pm)$ in Eq. (3.14) behaves qualitatively different for spheres as compared with cylinders (see Sec. II C) we treat them separately.

First, we consider the sphere, i.e., $d = D$, for which Eq. (2.31) holds for the behavior of $P_\pm(x_\pm, y_\pm \to 0)$ if $x_\pm > 0$ is fixed. However, the integral in Eq. (3.14) starts at the lower bound $x_\pm = 0$ where this condition for $x_\pm$ is violated. Therefore we temporarily split the $x_\pm$ integration into the intervals $0 < x_\pm < \sqrt{y_\pm}$ and $x_\pm > \sqrt{y_\pm}$. In the latter interval the relation $s/R > y_\pm^{-1/2} \to \infty$ holds so that Eq. (2.31) is applicable. This leads to [the curly brackets correspond to those in Eq. (3.14)]

$$y_\pm^{d-1} G_\pm(y_\pm) \to \int_0^{\sqrt{y_\pm}} dx_\pm \{\ \} + \int_{\sqrt{y_\pm}}^\infty dx_\pm [(x_\pm + y_\pm)^{D-1} [c_\pm (2y_\pm)^{\beta/\nu} x_\pm^{-2\beta/\nu} \mathcal{F}_\pm(x_\pm)] - y_\pm^{D-1} [P_\pm(x_\pm) - P_{\pm,b}]]. \qquad (3.15)$$

In the second integral the variable $y_\pm$ in $(x_\pm + y_\pm)^{D-1}$ can be replaced by zero in leading order for $y_\pm \to 0$ and the term proportional to $y_\pm^{D-1}$, i.e., the half-space contribution, can be dropped since $D - 1 > \beta/\nu$. The resulting integrand is integrable for $x_\pm \to 0$ so that the lower bound $\sqrt{y_\pm}$ can be replaced by zero and one can readily show that the resulting second integral in Eq. (3.15) dominates the first integral for $y_\pm \to 0$. This leads to the final result

$$G_\pm(y_\pm \to 0) \to \omega_\pm\, y_\pm^{-D+1+\beta/\nu}, \quad d = D, \qquad (3.16)$$

with the universal amplitudes

TABLE III. Numerical values of the universal amplitudes $\omega_\pm$ and $v_\pm$ [see Eqs. (3.17) and (3.21)] as presently available.

D	ω_+	ω_-	v_+	v_-
4	$4\sqrt{2}\simeq 5.657$	8	1.90	1.86
3	1.53 ± 0.05	$\simeq 1.47$		
2	0.515	0.0501	not defined	not defined

$$\omega_\pm = c_\pm\, 2^{\beta/\nu} \int_0^\infty dx_\pm\, x_\pm^{D-1-2\beta/\nu}\ \mathcal{F}_\pm(x_\pm). \quad (3.17)$$

The numerical values of $\omega_\pm$ for several spatial dimensions D as presently available are summarized in Table III (see Sec. IV B and Appendix B). Using Eq. (3.1) in conjunction with Eq. (2.24) yields

$$\Gamma(t\to 0,R)\to \mathcal{E}_{D,D}\, R^{\beta/\nu}\, \chi_b(t)\sim |t|^{-\gamma},\ \ d=D, \quad (3.18)$$

with the bulk susceptibility $\chi_b(t)\sim|t|^{-\gamma}$ and the critical exponent $\gamma = D\nu - 2\beta$. Equation (3.18) is, of course, consistent with Eqs. (3.16) and (3.7). For $t\to 0$ the universal function $R_\Phi(|t|,y_+,y_-)$ in Eq. (3.9) approaches the universal number

$$R_\Phi(0,0,0) = \lim_{t\to 0}\frac{\Gamma(+|t|,R)}{\Gamma(-|t|,R)} = \left(\frac{\xi_0^+}{\xi_0^-}\right)^{D-\beta/\nu}\frac{\omega_+}{\omega_-},\ \ d=D. \quad (3.19)$$

Whereas the dependence of the function $R_\Phi(|t|,y_+,y_-)$ on y_+, y_- is universal but depends on the definition used for the correlation length, we note that the limit $R_\Phi(0,0,0)$ in Eq. (3.19) is independent of the definition for the correlation length. The reason is that according to the first parts of Eqs. (3.19) and (3.1) $R_\Phi(0,0,0)$ can be expressed in terms of the order parameter profile $\langle\Phi(\mathbf{r})\rangle_t$ without resorting to the notion of the correlation length at all. (The same holds for the number R_Φ in Eq. (3.10) [14].)

Next, we consider the cylinder, i.e., $d=2$ and $D\geqslant 3$, which represents a relevant perturbation (see Sec. II C). In this case Eq. (2.35) holds for the behavior of $P_\pm(x_\pm, y_\pm \to 0)$. Thus $y_\pm^{d-1} G_\pm(y_\pm) = y_\pm\, G_\pm(y_\pm)$ becomes independent of $y_\pm$ in the limit $y_\pm\to 0$ and tends to the constant given by the integral in Eq. (3.14) with $y_\pm$ replaced by zero. This leads to

$$G_\pm(y_\pm\to 0)\to v_\pm\, y_\pm^{-1},\ \ d=2,\ \ D\geqslant 3, \quad (3.20)$$

with the universal numbers

$$v_\pm = \int_0^\infty dx_\pm\, x_\pm\,[N_\pm(x_\pm) - P_{\pm,b}]. \quad (3.21)$$

Numerical values of $v_\pm$ are only known for $D=4$ at present (see Table III and Sec. IV B). Note that the numbers $v_\pm$ are not defined for $D=2$ (compare Sec. II C). The exponent in the power law in Eq. (3.20) differs from that in Eq. (3.16)—apart from the difference generated on purely geometric grounds—by β/ν due to the different small $y_\pm$ behavior of the critical adsorption profiles for spheres as compared with cylinders. Equation (3.20) in conjunction with Eq. (3.7) leads to

$$\Gamma(t\to 0,R)\sim |t|^{\beta-2\nu},\ \ d=2,\ \ D\geqslant 3. \quad (3.22)$$

For $t\to 0$ the universal function $R_\Phi(|t|,y_+,y_-)$ in Eq. (3.9) tends to the universal number

$$R_\Phi(0,0,0) = \lim_{t\to 0}\frac{\Gamma(+|t|,R)}{\Gamma(-|t|,R)} = \left(\frac{\xi_0^+}{\xi_0^-}\right)^2\frac{v_+}{v_-},\ \ d=2,\ \ D\geqslant 3, \quad (3.23)$$

with $v_\pm$ given by Eq. (3.21). Again, the limit $R_\Phi(0,0,0)$ is independent of the definition for the correlation length [compare Eq. (3.19)].

IV. MEAN-FIELD THEORY

The critical fluctuations of the fluid are described by the standard Hamiltonian [7,8]

$$\mathcal{H}\{\Phi\} = \int_V dV\left\{\frac{1}{2}(\nabla\Phi)^2 + \frac{\tau}{2}\Phi^2 + \frac{u}{24}\Phi^4\right\} \quad (4.1)$$

for a scalar order parameter field $\Phi(\mathbf{r})$ supplemented by the boundary condition $\Phi=+\infty$ at the surface of the sphere or the cylinder corresponding to the critical adsorption fixed point [12]. The position vector $\mathbf{r}\in\mathbb{R}^D$ covers the volume $V = \mathbb{R}^D\backslash K$ accessible to the critical fluid. The parameter τ is proportional to $t=(T-T_c)/T_c$ and u is the Φ^4 coupling constant. The thermal average $\langle\Phi(\mathbf{r})\rangle$ corresponding to the Hamiltonian in Eq. (4.1) with the boundary condition for critical adsorption at the surface of K can be systematically expanded in terms of increasing powers of u, i.e.,

$$\langle\Phi(\mathbf{r})\rangle = \sqrt{\frac{6}{u}}\ [m(s;R,\tau)+\mathcal{O}(u)],\ \ s=r_\perp - R. \quad (4.2)$$

The leading contribution to this expansion corresponds to the mean-field result for the order parameter profile which becomes exact in the limit $D\nearrow 4$. The profile $m(s;R,\tau)$ is determined by minimizing $\mathcal{H}\{\Phi\}$ which leads to the Ginzburg-Landau type equation of motion

$$m''(s) + \frac{d-1}{s+R}m'(s) - \tau\, m(s) = m^3(s), \quad (4.3)$$

which is supplemented by the boundary conditions [7,8]

$$m(s\to 0;R,\tau)\to\frac{\sqrt{2}}{s}, \quad (4.4a)$$

$$m(s\to\infty;R,\tau)\to m_{\pm,b} = \begin{cases} 0, & \tau\geqslant 0,\\ |\tau|^{1/2}, & \tau<0. \end{cases} \quad (4.4b)$$

The parameter τ is related to $t=(T-T_c)/T_c$ and to the correlation length $\xi_\pm$ by

$$\xi_\pm = \xi_0^\pm\,|t|^{-1/2} = \begin{cases} \tau^{-1/2}, & \tau>0,\\ \dfrac{1}{\sqrt{2}}|\tau|^{-1/2}, & \tau<0, \end{cases} \quad (4.5)$$

and [compare the text following Eq. (2.2)]

$$a|t|^{1/2}=\sqrt{\frac{6}{u}}\,|\tau|^{1/2},\quad \tau<0. \tag{4.6}$$

Equations (4.3) and (4.4) uniquely determine the profile $m(s;R,\tau)$. The universal scaling functions $P_{\pm}(x_{\pm},y_{\pm})$ in Eq. (2.1) then read

$$P_{\pm}(x_{\pm},y_{\pm})=|\tau|^{-1/2}\,m(s;R,\tau),\quad D=4. \tag{4.7}$$

Within the present mean-field approach this scaling form holds because the LHS of Eq. (4.7) is dimensionless so that it depends only on the dimensionless variables $s|\tau|^{1/2}$ and $R|\tau|^{1/2}$, where $|\tau|^{1/2}$ is related to $\xi_{\pm}$ by Eq. (4.5). Similarly, the universal scaling function $\mathcal{C}_{+}(\Delta)$ in Eq. (2.11) is given by

$$\mathcal{C}_{+}(\Delta)=s\,m(s;R,\tau=0),\quad D=4. \tag{4.8}$$

Equations (4.7) and (4.8) lead to exact results for $D\nearrow 4$ and generalized cylinders K with arbitrary d in the interval $1\leqslant d\leqslant D$ (compare Fig. 3). Equations (4.3) and (4.4) can be solved numerically, e.g., by means of a shooting method [42]. In some cases analytical solutions are available. In the remaining part of this section we present the corresponding explicit results for the problems discussed in Secs. II and III.

A. Order parameter profiles

We start with the universal scaling functions $P_{\pm}(x_{\pm},y_{\pm})$ according to Eqs. (4.7) and (4.3). Figure 5 shows their behavior as function of $x_{\pm}=s/\xi_{\pm}$ for various values of the parameter $y_{\pm}=R/\xi_{\pm}$ in the case of a sphere (i.e., $d=D$ with $D=4$, compare Sec. II C and Fig. 3). For our presentation we choose a scaled form which reflects the behavior of $P_{\pm}(x_{\pm}\to 0,y_{\pm})$ (compare the inset of Fig. 2; here $\beta/\nu=1$). Accordingly, the curves start at the mean-field values $c_{+}=\sqrt{2}$ and $c_{-}=2$ [see Eq. (2.23) and Table I], respectively, and decay exponentially for $x_{\pm}\to\infty$. In order to deal with the rapid decay of $P_{-}(x_{-}\to\infty,y_{-})-1$ for small values of y_{-} in the case $T<T_c$ we replace the function $U(x_{-})$ in Eq. (2.10) by

$$U(x_{-},y_{-})=\tanh\left(\frac{x_{-}^{2}}{x_{-}+1}\,\frac{y_{-}+1}{y_{-}}\right),\quad d=D=4, \tag{4.9}$$

so that $U(x_{-},\infty)=U(x_{-})$. We emphasize again that the function $U(x_{-},y_{-})$ is introduced only in order to facilitate an appropriate representation of $P_{-}(x_{-},y_{-})$ which reflects the behavior for both small and large values of x_{-} for all values of y_{-} (compare the discussion related to Fig. 2). The overall dependence of $P_{\pm}(x_{\pm},y_{\pm})$ on the parameter $y_{\pm}$ is in line with Eq. (2.31) and the related discussion. Starting from the half-space behavior for $y_{\pm}=\infty$ the profiles $P_{\pm}(x_{\pm},y_{\pm})-P_{\pm,b}$ decrease with decreasing $y_{\pm}$ for any fixed value of $x_{\pm}$ and vanish in the limit $y_{\pm}\to 0$.

This latter behavior for a sphere differs from the corresponding one for a cylinder (i.e., $d=2$ and $D=4$, compare Sec. II C and Fig. 3). Figure 6 shows the corresponding behavior of $P_{\pm}(x_{\pm},y_{\pm})$ for various values of $y_{\pm}$. For the presentation of $P_{-}(x_{-},y_{-})$ in the case of the cylinder the function $U(x_{-})=U(x_{-},\infty)$ is suitable for all values of y_{-}. The overall dependence on $y_{\pm}$ is characterized by the fact

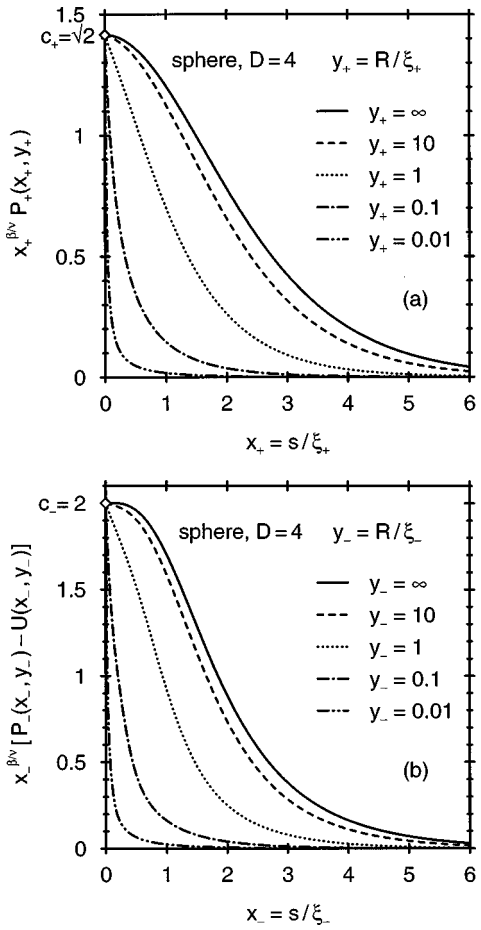

FIG. 5. (a) Scaling function $P_{+}(x_{+},y_{+})$ for a sphere in mean-field approximation (i.e., $d=D$ with $D=4$) as a function of x_{+} for several values of y_{+}. The curves start at the value c_{+} (compare the inset in Fig. 2). The curve for $y_{+}=\infty$ corresponds to the half-space profile [see Eq. (2.9)]. The curves decrease with decreasing y_{+} and vanish in the limit $y_{+}\to 0$. The slopes at $x_{+}=0$ can be read off from Eq. (4.16) with $s/R=x_{+}/y_{+}$. (b) Same representation for $P_{-}(x_{-},y_{-})$. The function $U(x_{-},y_{-})$ introduced for convenience is defined in Eq. (4.9).

that $P_{\pm}(x_{\pm},y_{\pm})$ does not vanish in the limit $y_{\pm}\to 0$ but rather tends to the finite limit function $P_{\pm}(x_{\pm},0)=N_{\pm}(x_{\pm})$ corresponding to the critical adsorption profile on a thin needle. This is in line with Eq. (2.35) and the related discussion. According to Eq. (2.36) the curves for $y_{\pm}=0$ start at the mean-field values of the universal amplitudes $n_{\pm}$ which are given by

$$n_{+}=1,\quad n_{-}=\sqrt{2},\quad D=4. \tag{4.10}$$

Next, we consider the universal scaling function $\mathcal{C}_{+}(\Delta)$ in Eq. (4.8) corresponding to $\tau=0$. Figure 7 shows its behavior for the present case $D=4$ and several values of d. The function $\mathcal{C}_{+}(\Delta)$ starts at $\mathcal{C}_{+}(0)=c_{+}$ [see the text following Eq. (2.12)] and for $\Delta\to\infty$ it vanishes in the case of the sphere (i.e., $d=D$ with $D=4$) while it tends to the finite number n_{+} from Eq. (4.10) in the case of the cylinder (i.e., $d=2$). In the marginal case $d=3$ it vanishes only logarithmically (compare Sec. II C and Fig. 3). For $\tau=0$ analytical solutions for Eq. (4.3) are available in some special cases even for $d>1$. For example, for $\tau=0$ and $d=4$ the differential equation can

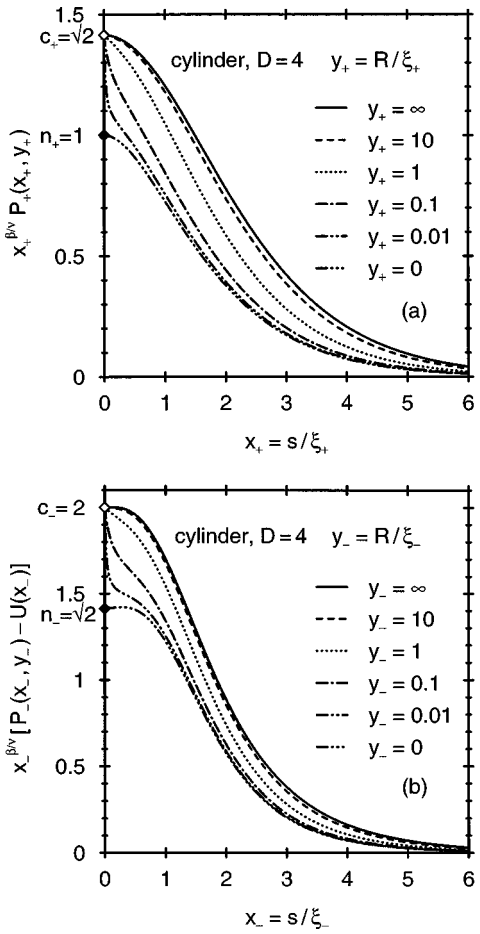

FIG. 6. (a) Scaling function $P_+(x_+,y_+)$ for a cylinder in mean-field approximation (i.e., $d=2$ and $D=4$) as a function of x_+ for several values of y_+ (compare Fig. 5). The curves decrease with decreasing y_+. In the limit $y_+\to 0$ they tend to the curve corresponding to $P_+(x_+,0)=N_+(x_+)$ describing the critical adsorption profile on a thin needle. The latter curve starts at the value n_+ (filled symbol). (b) Same representation for $P_-(x_-,y_-)$. The function $U(x_-)$ equals $U(x_-,\infty)$ from Eq. (4.9).

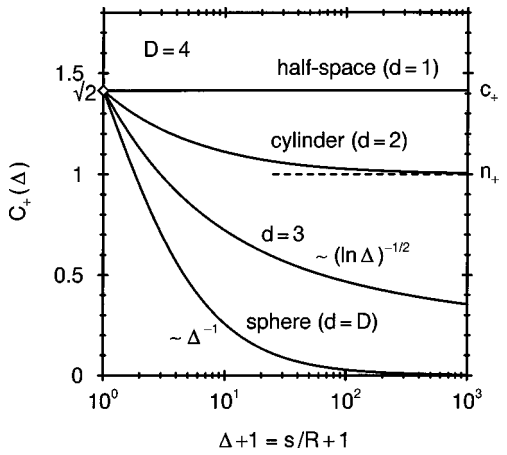

FIG. 7. Scaling function $\mathcal{C}_+(\Delta)$ in mean-field approximation (i.e., $D=4$) as a function of $\Delta=s/R$ for several values of d (compare Fig. 3). All curves start at the same value $\mathcal{C}_+(0)=c_+$ corresponding to the half-space but for large Δ the behaviors are qualitatively different. For a sphere $\mathcal{C}_+(\Delta\to\infty)$ vanishes as $\Delta^{-\beta/\nu}$ with $\beta/\nu=1$ whereas for a cylinder it tends to the finite value n_+. In the marginal case $d=3$ it vanishes only logarithmically.

be solved by relating it to the generalized Emden-Fowler equation [22], or by realizing that it represents a so-called ''equidimensional'' equation (see, e.g., Sec. 1.4 in Ref. [43]). The result is

$$m(s;R,\tau=0)=\frac{2\sqrt{2}\,R}{s\,(s+2R)},\quad d=4, \tag{4.11}$$

which agrees with Eqs. (4.8) and (2.15). It is worthwhile to note that an analytical solution also exists for the particular case $\tau=0$ and $d=5/2$ for which

$$m(s;R,\tau=0)=\frac{\sqrt{2}/2}{s+R-\sqrt{R\,(s+R)}},\quad d=5/2, \tag{4.12}$$

from which the corresponding result for $\mathcal{C}_+(\Delta)$ can be inferred from Eq. (4.8). Finally, for $\tau=0$, $R=0$, and arbitrary values of $d<3$ one finds

$$m(s;R=0,\tau=0)=\frac{\sqrt{3-d}}{s},\quad s=r_\perp,\quad d<3, \tag{4.13}$$

so that $\mathcal{C}_+(\infty)=n_+=\sqrt{3-d}>0$ for $d<3$. This is in line with Eq. (4.12) as well as with Fig. 3 and the related discussion, according to which in $D=4$ a generalized cylinder K with $d<3$ represents a relevant perturbation. In particular, Eq. (4.13) leads to $m(r_\perp)=1/r_\perp$ representing the mean-field profile near a thin needle (for which $d=2$, compare Sec. II C) at criticality. In Appendix A we calculate the corresponding two-point correlation function in the presence of this profile.

The asymptotic behavior of $P_\pm(x_\pm,y_\pm)$ for $D=4$ in various limiting cases can be derived directly from the defining Eqs. (4.7) and (4.3) even for those cases in which no full analytical solution is available [44].

(i) $x_\pm=s/\xi_\pm\gg 1$ with $y_\pm=R/\xi_\pm$ fixed. Because in this limit $m(s;R,\tau)-m_{\pm,b}$ is exponentially small, in Eq. (4.3) one can neglect powers of it larger than one. This leads to a linear differential equation for $m(s;R,\tau)-m_{\pm,b}$ which can be solved in terms of modified Bessel functions $K_\alpha(x_\pm+y_\pm)$ and $I_\alpha(x_\pm+y_\pm)$ [45] with index $\alpha=(d-2)/2$. Here only the decreasing function K_α must be considered. Using the asymptotic behavior of K_α for large arguments [45] and Eq. (4.7) one finds

$$P_\pm(x_\pm,y_\pm)-P_{\pm,b}\to A_\pm(y_\pm;d)\,(x_\pm+y_\pm)^{-\frac{d-1}{2}}\times\exp(-x_\pm),\quad x_\pm\gg 1, \tag{4.14}$$

where the amplitude function $A_\pm(y_\pm;d)$ remains undetermined by the present method and must be evaluated numerically in general. An important feature of Eq. (4.14) is that for increasing values of $x_\pm$ the exponential decay is enhanced by the algebraic prefactor. Thus the decay is weaker if $x_\pm\ll y_\pm$ and it is weaker for a cylinder ($d=2$) than for a sphere ($d=D$ with $D=4$). This is expected because the perturbation of the bulk fluid is strongest in case of the half-space (corresponding to $x_\pm\ll y_\pm$), less for a cylinder, and even less for a sphere.

(ii) $x_\pm \to 0$ with R and $\xi_\pm$ fixed, i.e., $s \to 0$ (compare Sec. II B). The leading behavior of $m(s \to 0; R, \tau)$ can be obtained by inserting the ansatz

$$m(s;R,\tau) = \frac{\sqrt{2}}{s} + a_0 + a_1 s + \mathcal{O}(s^2) \tag{4.15}$$

into Eq. (4.3) and fixing the coefficients a_0 and a_1 such that the prefactors of the most singular powers of s cancel. The resulting expression can be arranged so that it takes the form implied by Eqs. (2.23) and (4.7), i.e.,

$$m(s\to 0;R,\tau) = \frac{\sqrt{2}}{s}\left\{1 - \frac{1}{3}\frac{d-1}{2}\frac{s}{R} + \left[\frac{5}{9}\frac{(d-1)^2}{4} - \frac{1}{3}\frac{(d-1)(d-2)}{2}\right]\frac{s^2}{R^2} - \frac{1}{6}\tau s^2 + \cdots\right\}. \tag{4.16}$$

Equation (4.16) confirms that the leading dependence on τ is analytic with the same prefactor as for the half-space. In addition, one can read off the curvature parameters according to mean-field theory, i.e.,

$$\kappa_1 = -\frac{1}{3}, \quad \kappa_2 = \frac{5}{9}, \quad \kappa_G = -\frac{1}{3}, \quad D = 4. \tag{4.17}$$

We note that the derivation of Eq. (4.16) implicitly contains a consistency check for the validity of the general curvature expansion (2.23). For example, the parameters κ_2 and κ_G are fixed by considering only two different types of generalized cylinders K with nonvanishing curvature, e.g., those for which $d=2$ and $d=3$. Equation (4.17), however, holds for any value of d in the interval $1 \leqslant d \leqslant D$ with $D=4$ which encompasses, in particular, the three integer values $d=2$, 3, and 4 (compare Fig. 3). Thus the curvature parameters are overdetermined. In the present case, however, this consistency may be regarded as a simple consequence of the differential equation (4.3) in which the perturbation generated by the surface curvature is proportional to $d-1$. In the next subsection we consider the small curvature expansion (3.12) for the excess adsorption, for which the corresponding consistency check in $D=4$ provides a more stringent test.

(iii) $y_\pm \to 0$ with s and $\xi_\pm$ fixed, i.e., $R \to 0$ (compare Sec. II C). We consider the case of a sphere, i.e., $d=D$ with $D=4$. By inserting the ansatz $m(s;R,\tau) - m_{\pm,b} = R\, u(s;\tau)$ into Eq. (4.3) and keeping only terms linear in R one obtains a linear differential equation for $u(s;\tau)$, similar to case (i) above. The solution of this differential equation in terms of the modified Bessel function $K_1(x_\pm)$ [45] in conjunction with Eq. (4.7) leads to

$$P_\pm(x_\pm, y_\pm \to 0) - P_{\pm,b} \to 2c_\pm y_\pm x_\pm^{-1} K_1(x_\pm), \quad d = D = 4. \tag{4.18}$$

Here the constant prefactor $2c_\pm$ is fixed because the limit $x_\pm \to 0$ of the RHS of Eq. (4.18) must reproduce Eq. (2.12), in which $\mathcal{C}_\pm(\Delta \to \infty) \to 2c_\pm/\Delta$ for $d=D=4$ according to Eq. (2.15). Equation (4.18) is in line with Eq. (2.31) because for $D=4$ one has $\beta/\nu = 1$ and the universal scaling functions $\mathcal{F}_\pm(x_\pm)$ are given by

$$\mathcal{F}_\pm(x_\pm) = x_\pm K_1(x_\pm), \quad D = 4. \tag{4.19}$$

B. Excess adsorption

For $D=4$ Eq. (3.7) reduces to

$$\Gamma(t \to 0, R) \to A\, a\, \xi_0^\pm \{g_\pm |\ln|t||\, + G_\pm(y_\pm)\}, \quad D = 4, \tag{4.20}$$

with $g_+ = 1/\sqrt{2}$ and $g_- = 1$. The universal scaling function $G_\pm(y_\pm)$ in Eq. (4.20) is given by Eq. (3.6) with $P_\pm(x_\pm, y_\pm)$ and $P_\pm(x_\pm)$ from Eqs. (4.7) and (2.9). In the following we discuss the behavior of $G_\pm(y_\pm)$ in the limit of large and small values of $y_\pm = R/\xi_\pm$ and give results for the whole range of $y_\pm$ representing the crossover between these two limits.

(i) $G_\pm(y_\pm)$ for $y_\pm \to \infty$ (compare Sec. III B). By using the differential equation (4.3) in conjunction with Eq. (4.7) one can determine the coefficients $a_{d,D}^\pm$ and $b_{d,D}^\pm$ in Eq. (3.11) for generalized cylinders K with $D=4$ and arbitrary d in the interval $1 \leqslant d \leqslant 4$. This calculation is presented in Appendix C. As a result one finds that the dependences of $a_{d,4}^\pm$ and $b_{d,4}^\pm$ on d are precisely of the form given by Eq. (3.13). In the present case $D=4$ one has $|t|^{\beta-\nu} = 1$ and the curvature parameters are given by [46]

$$\lambda_1^+ = 5.09\ \xi_+, \quad \lambda_1^- = 4.91\ \xi_-, \tag{4.21a}$$

$$\lambda_2^+ = -1.55\ \xi_+^2, \quad \lambda_2^- = -0.91\ \xi_-^2, \tag{4.21b}$$

$$\lambda_G^+ = 2.87\ \xi_+^2, \quad \lambda_G^- = 2.52\ \xi_-^2. \tag{4.21c}$$

The consistency with Eq. (3.13) for $D=4$ can be traced back to nontrivial properties of the differential equation (4.3) (see Appendix C) and thus provides an important check for the validity of the general curvature expansion (3.12). We expect that the curvature expansion (3.12) is also valid in $D=3$ and that the corresponding numerical prefactors multiplying ξ or ξ^2 in the curvature parameters for $D=3$ differ only quantitatively from those in Eq. (4.21) valid for $D=4$.

As an illustration, consider a curved *membrane* with both sides exposed to a fluid near criticality. In particular we consider the *total* excess adsorption, i.e., the sum of the excess adsorptions on each side of the membrane, per unit area. In this case the contributions to $\lambda_1^\pm K_m$ in the expansion (3.12) from each side cancel and the signs in Eqs. (4.21b) and (4.21c) in conjunction with Eq. (2.21) imply that the total excess adsorption is *larger* near spherical regions ($d=D$) of the membrane as compared to flat regions, whereas near cylindrical regions ($d=2$) it is *smaller* as compared to flat regions.

(ii) $G_\pm(y_\pm)$ for $y_\pm \to 0$ (compare Sec. III C). In this case the behaviors for spheres and cylinders are qualitatively different due to the different behaviors of $P_\pm(x_\pm, y_\pm)$. For a sphere (i.e., $d=D$ with $D=4$) the power law (3.16) is valid where the exponent $-D+1+\beta/\nu$ equals -2 and according to Eqs. (3.17) and (4.19) the universal amplitudes $\omega_\pm$ are given by

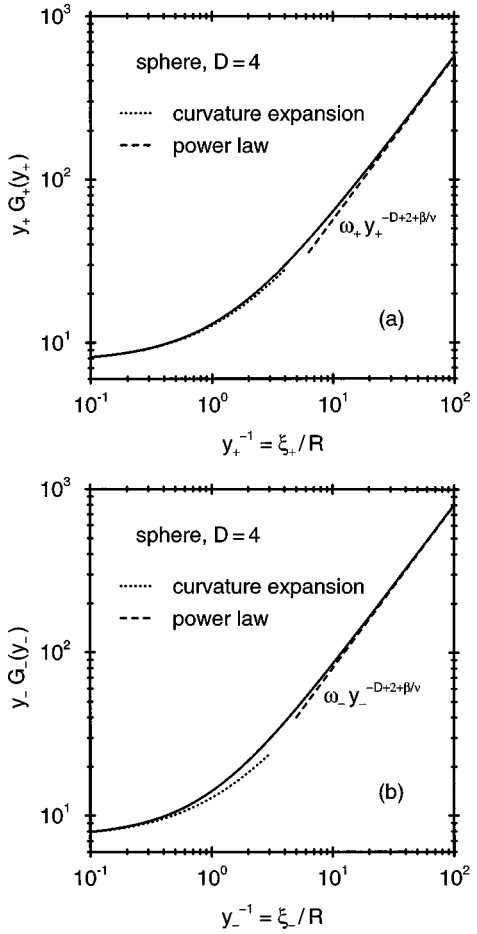

FIG. 8. Scaling functions $G_\pm(y_\pm)$ for a sphere in mean-field approximation (i.e., $d=D$ with $D=4$) as a function of $y_\pm^{-1} = \xi_\pm/R$ for (a) $T>T_c$ and (b) $T<T_c$. The dotted lines show the small curvature expansion [see Eqs. (3.11)–(3.13), and (4.21)] valid for $y_\pm^{-1} \ll 1$ and the dashed lines show the power law [see Eqs. (3.16) and (4.22)] valid for $y_\pm^{-1} \to \infty$; for $D=4$ the exponent $-D+2+\beta/\nu$ is equal to -1.

$$\omega_+ = 4\sqrt{2}, \quad \omega_- = 8, \quad d = D = 4. \tag{4.22}$$

For a cylinder (i.e., $d=2$ and $D=4$) one finds the behavior (3.20) where the universal numbers $\upsilon_\pm$ in Eq. (3.21) can be evaluated numerically with the result

$$\upsilon_+ = 1.90, \quad \upsilon_- = 1.86, \quad d = 2, \quad D = 4. \tag{4.23}$$

(iii) The full scaling functions $G_\pm(y_\pm)$ describe the crossover between their analytic behaviors for $y_\pm = R/\xi_\pm \to \infty$ and the power laws for $y_\pm \to 0$ which have been discussed in (i) and (ii) above. Figures 8 and 9 show numerical results for $G_\pm(y_\pm)$ corresponding to a sphere and a cylinder, respectively, in $D=4$. The results confirm the small curvature expansion as implied by Eqs. (3.11)–(3.13) and (4.21) and the properties (3.16) and (3.20), and they provide the range of validity of the asymptotic behavior. Note that in the case of the sphere $y_\pm G_\pm(y_\pm)$ as function of $y_\pm^{-1} = \xi_\pm/R$ diverges for $y_\pm^{-1} \to \infty$ with the corresponding power law whereas in the case of the cylinder with increasing $y_\pm^{-1}$ it interpolates between one finite value related to $\lambda_1^\pm$ to the other finite value $\upsilon_\pm$.

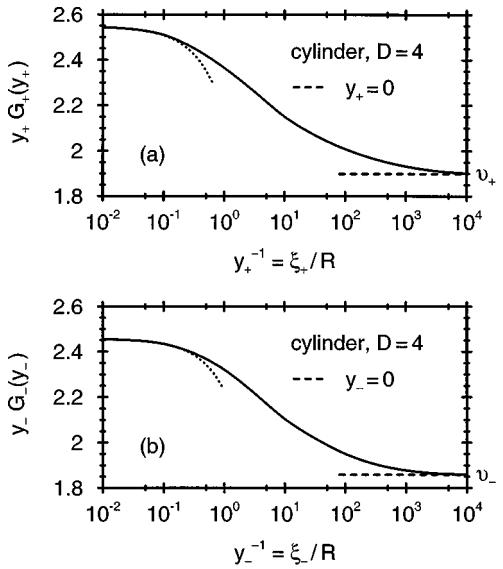

FIG. 9. Scaling functions $G_\pm(y_\pm)$ for a cylinder in mean-field approximation (i.e., $d=2$ and $D=4$) as a function of $y_\pm^{-1} = \xi_\pm/R$ for (a) $T>T_c$ and (b) $T<T_c$ (compare Fig. 8). The dotted lines show the small curvature expansion and the dashed lines correspond to the numbers $\upsilon_\pm$ in the behavior $G_\pm(y_\pm \to 0) \to \upsilon_\pm y_\pm^{-1}$ [see Eqs. (3.20) and (4.23)].

V. SUMMARY AND CONCLUDING REMARKS

We have studied critical adsorption phenomena on spherical and cylindrical particles of radius R which are immersed in a fluid near criticality, $t=(T-T_c)/T_c \to 0$, for the case that the fluid is at the critical composition. The corresponding adsorption profiles at the radial distance s from the surface are characterized by universal scaling functions $P_\pm(s/\xi_\pm, R/\xi_\pm)$ for $T \neq T_c$, involving the bulk correlation lengths $\xi_\pm$ for $T \gtrless T_c$, and $\mathcal{C}_+(s/R)$ for $T=T_c$ [see Eqs. (2.1) and (2.11), respectively].

In the following we summarize our main results starting with *local properties* of $P_\pm(x_\pm, y_\pm)$ and $\mathcal{C}_+(\Delta)$ in various limiting cases as indicated by Fig. 4.

(1) For $T=T_c$ we have introduced the short distance expansion of the order parameter profile near a weakly curved $(D-1)$-dimensional surface of *general* shape [see Eq. (2.18)]. This expansion involves the local curvature invariants K_m, K_m^2, and K_G [see Eq. (2.17)]. The corresponding expansion parameters κ_1, κ_2, and κ_G appear also in the short distance expansion (2.23) of $P_\pm(x_\pm, y_\pm)$ valid for $T \gtrless T_c$. The parameters κ_1, κ_2, and κ_G are universal and depend only on the space dimension D [see Eqs. (2.19), (2.20), and (4.17)].

(2) For $R \ll s, \xi$ the order parameter profile near a cylinder becomes independent of R in the limit $R \to 0$, i.e., if the cylinder radius is microscopically small [see Eqs. (2.33)–(2.36)]. In contrast, near a sphere the universal part of the order parameter profile, i.e., the one described by Eqs. (2.30) and (2.31), vanishes for $R \to 0$. This *qualitative* difference in behavior can be explained by means of a small radius operator expansion [see Eqs. (2.24) and (2.25)]. As indicated by Fig. 3 a sphere is an irrelevant perturbation for the fluid near criticality whereas a cylinder is a relevant perturbation.

(3) The explicit forms of the universal scaling functions $P_\pm(x_\pm, y_\pm)$ and $\mathcal{C}_+(\Delta)$ for a sphere and a cylinder within

mean-field approximation (see Figs. 5–7) corroborate the results described in (1) and (2) above.

We now turn to the *excess adsorption* $\Gamma(t\to 0,R)$ describing the total enrichment of the preferred component of the fluid near criticality in proximity of a sphere or cylinder [see Eq. (3.1)]. The curvature dependence of $\Gamma(t\to 0,R)$ is characterized by universal scaling functions $G_{\pm}(R/\xi_{\pm})$ obtained from $P_{\pm}(s/\xi_{\pm},R/\xi_{\pm})$ by integrating over the first variable $s/\xi_{\pm}$ [see Eqs. (3.6) and (3.7)].

(4) For $R/\xi_{\pm}\gg 1$ we have introduced the expansion of $\Gamma(t\to 0,R)$ near a weakly curved $(D-1)$-dimensional surface of *general* shape in terms of the local curvature invariants K_m, K_m^2, and K_G [see Eq. (3.12)]. The corresponding expansion parameters $\lambda_1^{\pm}$, $\lambda_2^{\pm}$, and $\lambda_G^{\pm}$ depend only on the space dimension D and can be expressed in terms of the universal coefficients $a_{d,D}^{\pm}$ and $b_{d,D}^{\pm}$ appearing in the expansion of $G_{\pm}(y_{\pm}\to\infty)$ [see Eqs. (3.11)–(3.13)]. The explicit calculation of $\lambda_1^{\pm}$, $\lambda_2^{\pm}$, and $\lambda_G^{\pm}$ within mean-field approximation [see Eq. (4.21) and Appendix C] provides an important check for the validity of the general curvature expansion of the excess adsorption.

(5) For $R/\xi_{\pm}\to 0$ the behaviors of $\Gamma(t\to 0,R)$ and $G_{\pm}(y_{\pm})$ are characterized by power laws [see Eqs. (3.16)–(3.18) for a sphere and (3.20)–(3.22) for a cylinder]. The exponents in these power laws are different for spheres and cylinders beyond the purely geometrical effects. This can be traced back to the corresponding difference in behavior of $P_{\pm}(x_{\pm},y_{\pm})$ addressed in (2).

(6) The explicit forms of $G_{\pm}(y_{\pm})$ for a sphere and a cylinder in mean-field approximation (see Figs. 8 and 9) confirm the general results presented in (4) and (5).

We conclude by summarizing some of the *field-theoretical developments* and *perspectives* for future theoretical work, simulations, and experiments.

(7) For a systematic field-theoretical analysis of the critical adsorption phenomena on spheres and cylinders it is useful to introduce the particle shape of a ''generalized cylinder'' [see Eq. (1.1) and Fig. 1] which is characterized by the space dimension D and an internal dimension d encompassing a sphere, a cylinder, and a planar wall as special cases.

(8) For a single sphere, certain asymptotic behaviors of the order parameter *profile* are characterized by universal quantities [see Eqs. (2.23) and (2.31)]. These quantities are accurately known in $D=3$ [see Eqs. (2.19), (2.20), and Table I; as far as the scaling functions $\mathcal{F}_{\pm}(x_{\pm})$ are concerned, only the function $\mathcal{F}_{+}(x_{+})$ appropriate for $T>T_c$ is known accurately for $D=3$, see Appendix B]. The corresponding predictions can be tested using small angle scattering of light, X-rays, or neutrons which can probe the enlarged effective size of the colloidal particles due to the adsorption.

(9) For a single sphere, in $D=3$ the behavior of the *excess adsorption* in the limit $R/\xi_{\pm}\to 0$ is available as well [see Eqs. (3.7), (3.16)–(3.18), and Table III] and can be tested experimentally by, e.g., volumetric measurements. For a disc in $D=2$ the numerical values of the universal amplitudes $\omega_{\pm}$ in Eq. (3.16) are also known (compare Appendix B). This can be relevant for protein inclusions in fluid membranes [47].

(10) Apart from the curvature dependence of the excess adsorption [see Eq. (3.12)] also the corresponding energetic contributions, i.e., the change of the surface tension generated by the surface curvature, can be relevant for applications. For example, in case of a membrane immersed in a fluid near criticality such contributions and their temperature dependence are expected to influence the intrinsic bending rigidities of the membrane. These modifications of the bending rigidities can, in turn, induce shape changes of vesicles formed by closed membranes in a controllable way (see, e.g., Ref. [48]).

(11) A one-dimensional extended perturbation in an Ising-like system which breaks the symmetry of the order parameter represents a relevant perturbation (see Sec. II C) of the bulk system. This gives rise to new universal quantities such as the critical exponents $\eta_{\|}$ and $\eta_{\perp}$ characterizing the decay of the structure factor [see Appendix A and in particular Eqs. (A9) and (A11)] and the amplitudes $n_{\pm}$ and $v_{\pm}$ [see Eqs. (2.36) and (3.21), respectively; the mean-field values of $n_{\pm}$ and $v_{\pm}$ are quoted in Eqs. (4.10) and (4.23)]. Apart from a rodlike particle immersed in a fluid, such a one-dimensional perturbation could also be realized in a *solid*, e.g., by a lattice dislocation in a binary alloy if the dislocation locally breaks the symmetry of the order parameter. This would be a natural starting point for testing the numerous field-theoretical predictions derived here by Monte Carlo simulation.

(12) As stated in the Introduction, the results addressed in (2) can be relevant for the flocculation of colloidal particles dissolved in a fluid near criticality. Specificly, if one considers the case $T=T_c$ and compares the behaviors of the order parameter profiles near a sphere and near an infinitely elongated cylinder, respectively, the order parameter of the fluid at a distance $s\gg R$ from the particle with radius R is larger by a factor $\sim(s/R)^{\beta/\nu}\gg 1$ for the cylinder than for the sphere [see Eqs. (2.11), (2.30), and (2.33)]. For rods with a large but finite length l and distances $s\gtrsim l$ this enhancement is of the order of $(l/R)^{\beta/\nu}\gg 1$. Since the critical Casimir forces between particles are partially induced by an overlap of the order parameter profiles generated by the individual particles in the space between them, the aforementioned results suggest that not only spheres but, *a fortiori*, also long rods in a fluid near criticality can aggregate due to critical Casimir forces.

ACKNOWLEDGMENTS

We thank Professor E. Eisenriegler for helpful discussions and Professor A. J. Bray and Professor M. E. Fisher for helpful correspondence. This work has been supported by the German Science Foundation through Sonderforschungsbereich 237 *Unordnung und große Fluktuationen.*

APPENDIX A: TWO-POINT CORRELATION FUNCTION NEAR A NEEDLE

The two-point correlation function $G(\mathbf{r},\mathbf{r}')$ for Gaussian fluctuations around the profile $m(r_{\perp})=1/r_{\perp}$ [see the text following Eq. (4.13)] *at* criticality satisfies the differential equation

$$[-\Delta_D+3\,m^2(r_{\perp})]\,G(\mathbf{r},\mathbf{r}')=\delta^{(D)}(\mathbf{r}-\mathbf{r}'), \qquad \text{(A1)}$$

where Δ_D is the Laplacian operator in D-dimensional space. (Although the present mean-field calculation implies $D=4$

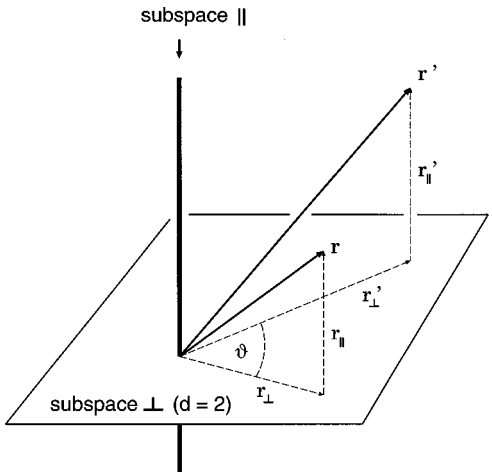

FIG. 10. A thin ''needle'' corresponding to a generalized cylinder K with $d=2$ and $R=0$ [compare Eq. (1.1) and Fig. (1)]. The two spatial arguments $\mathbf{r}$ and $\mathbf{r}'$ of the correlation function in Eq. (A4) are also shown.

we leave the symbol D for clarity.) In coordinates adapted to the geometry of a generalized cylinder K with $d=2$ and $R=0$ the Laplacian operator Δ_D has the form

$$\Delta_D=\Delta_\perp+\sum_{i=1}^{D-2}\frac{\partial^2}{\partial r_{\|,i}^{\,2}} \tag{A2}$$

with

$$\Delta_\perp=\frac{\partial^2}{\partial r_\perp^{\,2}}+\frac{1}{r_\perp}\frac{\partial}{\partial r_\perp}+\frac{1}{r_\perp^{\,2}}\frac{\partial^2}{\partial\vartheta^2} \tag{A3}$$

as the Laplacian operator in the two-dimensional subspace perpendicular to K. Here ϑ denotes the angle between $\mathbf{r}_\perp$ and a fixed direction in the radial subspace. In order to solve Eq. (A1) we carry out the Fourier transform in the subspace parallel to K and a partial wave decomposition in the radial subspace, i.e.,

$$\begin{aligned}G(\mathbf{r},\mathbf{r}')&=G(r_\perp,r_\perp',\vartheta,|\mathbf{r}_\|-\mathbf{r}_\|'|)\\&=\sum_{n=0}^{\infty}W_n(\vartheta)\int\frac{d^{D-2}p}{(2\pi)^{D-2}}\exp[i\,\mathbf{p}\cdot(\mathbf{r}_\|-\mathbf{r}_\|')]\\&\quad\times\tilde{G}_n(r_\perp,r_\perp',p),\end{aligned} \tag{A4}$$

where ϑ is now the angle between $\mathbf{r}_\perp$ and $\mathbf{r}_\perp'$ (see Fig. 10). The functions $W_n(\vartheta)$ are given by

$$W_n(\vartheta)=\frac{2-\delta_{n,0}}{2\pi}\cos(n\vartheta) \tag{A5}$$

with $\delta_{n,0}=1$ for $n=0$ and zero otherwise. They obey $\Sigma_n W_n(\vartheta)=\delta(\vartheta)/2$ where the support of the δ-function on the RHS is located entirely in the interval $\vartheta\geqslant 0$ so that $\int_0^{\vartheta'}d\vartheta\,\delta(\vartheta)=1$ for any $\vartheta'>0$. The propagator $\tilde{G}_n$ in Eq. (A4) satisfies the radial equation

$$\left[-\frac{\partial^2}{\partial r_\perp^{\,2}}-\frac{1}{r_\perp}\frac{\partial}{\partial r_\perp}+p^2+\frac{n^2+3}{r_\perp^{\,2}}\right]\tilde{G}_n(r_\perp,r_\perp',p)=\frac{\delta(r_\perp-r_\perp')}{r_\perp}. \tag{A6}$$

For $r_\perp\neq r_\perp'$ the solutions of this equation are modified Bessel functions $K_\lambda(p\,r_\perp)$ and $I_\lambda(p\,r_\perp)$ [45] with index

$$\lambda=\lambda_n=\sqrt{n^2+3}. \tag{A7}$$

The physically acceptable solution $\tilde{G}_n$ of Eq. (A6) is uniquely determined by the requirements that (i) it is symmetric in $r_\perp$ and $r_\perp'$, (ii) it decays for $r_\perp\to\infty$, and (iii) it does not diverge as the singularity at $r_\perp=0$ in Eq. (A6) is approached. The result is

$$\tilde{G}_n(r_\perp,r_\perp',p)=K_\lambda(p\,r_\perp^{(>)})\,I_\lambda(p\,r_\perp^{(<)}) \tag{A8}$$

with $r_\perp^{(>)}=\max(r_\perp,r_\perp')$, $r_\perp^{(<)}=\min(r_\perp,r_\perp')$, and λ given by Eq. (A7). Equations (A4) and (A8) represent the two-point correlation function near a thin needle in the presence of the adsorption profile $m(r_\perp)=1/r_\perp$ at criticality. In the following we infer the asymptotic behavior of $G(\mathbf{r},\mathbf{r}')$ in various limits.

(a) $r_\perp$, $r_\perp'$ fixed and $|\mathbf{r}_\|-\mathbf{r}_\|'|\to\infty$. The RHS of Eq. (A8) can be expanded for $p\to 0$, e.g., by relating K_λ to $I_{-\lambda}$ and I_λ via the corresponding formula in Sec. 9.6.2 of Ref. [45](a) and by using the formula in Sec. 9.6.10 of the same reference. Apart from terms proportional to integer powers of p^2, which are analytic in $\mathbf{p}$ yielding only exponentially decaying contributions on the LHS of Eq. (A4), one finds that the *leading singular* contribution behaves as $p^{2\lambda}$. Regarding the leading behavior for $|\mathbf{r}_\|-\mathbf{r}_\|'|\to\infty$ in Eq. (A4) only the term with $n=0$ is important so that

$$G(r_\perp,r_\perp',\vartheta,|\mathbf{r}_\|-\mathbf{r}_\|'|\to\infty)\sim\frac{1}{|\mathbf{r}_\|-\mathbf{r}_\|'|^{D-2+\eta_\|}} \tag{A9a}$$

with

$$\eta_\|=2\lambda_0=2\sqrt{3}. \tag{A9b}$$

(b) $\mathbf{r}_\|=\mathbf{r}_\|'$, $r_\perp'$ fixed and $r_\perp\to\infty$. For $r_\perp>r_\perp'$ using Eq. (A4) and rescaling $x=p\,r_\perp$ leads to

$$G(r_\perp,r_\perp',\vartheta,0)=\frac{1}{r_\perp^{D-2}}\sum_{n=0}^{\infty}W_n(\vartheta)\int\frac{d^{D-2}x}{(2\pi)^{D-2}}\times K_\lambda(x)\,I_\lambda(xr_\perp'/r_\perp). \tag{A10}$$

Here $I_\lambda(xr_\perp'/r_\perp)$ can be expanded for $r_\perp'/r_\perp\to 0$ so that in this limit again only the term with $n=0$ is important and

$$G(r_\perp\to\infty,r_\perp',\vartheta,0)\sim\frac{1}{r_\perp^{D-2+\eta_\perp}} \tag{A11a}$$

with

$$\eta_\perp = \lambda_0 = \sqrt{3}. \tag{A11b}$$

We note that within the present mean-field theory the relation $2\eta_\perp = \eta + \eta_\parallel$ is fulfilled because $\eta(D=4)=0$.

The exponents in Eqs. (A9) and (A11) for a needle are different from those for the half-space for which $\eta_\parallel^{\rm hs}=6$ and $\eta_\perp^{\rm hs}=3$ in mean-field approximation. Thus the correlations in the critical fluid are more suppressed in proximity of the needle than in the bulk fluid, and are even more suppressed near the surface bounding the half-space. This can be understood by noting that a needle represents a weaker, but still relevant, perturbation for the critical fluid than a planar wall (compare Fig. 3). For a sphere one finds that the two-point correlation function at criticality decays as $|\mathbf{r}-\mathbf{r}'|^{-(D-2+\eta)}$ with the bulk exponent η if the distance vector $\mathbf{r}-\mathbf{r}'$ is increased in any direction. This reflects the fact that a sphere represents an irrelevant perturbation.

APPENDIX B: AMPLITUDES $\omega_\pm$ AND SCALING FUNCTIONS $\mathcal{F}_\pm(x_\pm)$

In this appendix we determine the universal amplitudes $\omega_\pm$ [see Eqs. (3.16) and (3.17)] and the universal scaling functions $\mathcal{F}_\pm(x_\pm)$ [see Eqs. (2.31) and (2.32)]. The corresponding mean-field results [see Eqs. (4.22) and (4.19), respectively] hold in $D=4$. For $D=3$ and 2 results are available [49–54] for the Fourier transform of the bulk two-point correlation function introduced in Eq. (2.32), i.e.,

$$S_t(p) = \int d^D r\, e^{i\,\mathbf{p}\cdot\mathbf{r}} \langle \Phi(\mathbf{r})\Phi(0)\rangle_{b,\,t}^{C}, \tag{B1}$$

which can be written in the scaling form

$$S_t(p) = C^\pm\, |t|^{-\gamma} g_\pm(p\,\xi_\pm). \tag{B2}$$

The universal scaling functions $g_\pm(Y_\pm)$ are fixed by the normalization condition $g_\pm(0)=1$ and the choice of $\xi_\pm$ as the true correlation length for $T \gtrless T_c$. The nonuniversal amplitudes $C^\pm$ and the universal bulk critical exponent $\gamma = \nu(2-\eta)$ characterize the bulk susceptibility $\chi_b(t) = S_t(0) = C^\pm |t|^{-\gamma}$ in the critical regime $t \to 0$. Numerical values of the universal bulk critical exponent η are given by $\eta(D=2)=1/4$ and $\eta(D=3)=0.031$ [33] [compare Eq. (2.5)]. Inserting Eq. (2.32) into Eq. (B1) and using Eq. (3.17) yields

$$\omega_\pm = \frac{c_\pm\, 2^{\beta/\nu}}{\Omega_D\, \tilde{Q}_\pm} \tag{B3}$$

with $\Omega_D = 2\pi^{D/2}/\Gamma(D/2)$. The universal numbers $\tilde{Q}_\pm$ are given by

$$\tilde{Q}_\pm = \begin{cases} N\, R_+^{2-\eta} Q_3, & T > T_c, \\ N\, R_+^{2-\eta} R_\xi^{\eta-2} \dfrac{C^+}{C^-} Q_3, & T < T_c, \end{cases} \tag{B4}$$

with the universal amplitude ratio $Q_3 = \hat{D}\,(\xi_{0,1}^+)^{2-\eta}/C^+$ introduced by Tarko and Fisher [51]. The amplitudes $\xi_{0,1}^\pm$ correspond to correlation length defined via the second moment [51] of the correlation function, i.e., $\xi_{\pm,1} = \xi_{0,1}^\pm |t|^{-\nu}$. The amplitude $\hat{D}$ is defined by $S_{t=0}(p) = \hat{D}\, p^{\eta-2}$ which implies that B_Φ in Eq. (2.27) is related to $\hat{D}$ via $B_\Phi = N\hat{D}$ with the numbers

$$N = \begin{cases} \Gamma\left(\dfrac{1}{8}\right) \Big/ \left[2\pi\, 2^{3/4}\, \Gamma\left(\dfrac{7}{8}\right)\right] = 0.654308, & D=2, \\ \Gamma(\eta) \sin\left(\dfrac{\eta\pi}{2}\right) \Big/ (2\pi^2) = 0.078196, & D=3. \end{cases} \tag{B5}$$

Numerical values of Q_3 are given by $Q_3(D=2)=0.41377$ and $Q_3(D=3)=0.896$ [51]. In Eq. (B4) $R_+ = \xi_0^+/\xi_{0,1}^+$, $R_\xi = \xi_0^+/\xi_0^-$, and C^+/C^- are known universal amplitude ratios with $R_+(D=2)=1.000402$ [see Eq. (3.7) in Ref. [52]], $R_+(D=3)=1.0003$ [50], $R_\xi(2)=2$, $R_\xi(3)\simeq 1.92$ [50], $(C^+/C^-)(2)=37.693562$ [51], $(C^+/C^-)(3)=4.95$ [54]. Using Eqs. (B3) and (B4) in conjunction with the values of $c_\pm(D=2)$ from Table I and with $c_+(D=3)=0.94$, and $c_-(D=3)=1.24$ yields the values of $\omega_\pm$ quoted in Table III. We note that the accuracy of the quoted value of $\omega_-(D=3)$ is unknown because the accuracy of the aforementioned value of $R_\xi(D=3)$ is not given reliably [50].

Next we outline how the universal scaling functions $\mathcal{F}_\pm(x_\pm)$ introduced in Eq. (2.32) can be inferred from presently available results for $g_\pm(Y_\pm)$ [see Eqs. (B1) and (B2)].

(a) $D=3$. In this case the scaling functions $\mathcal{F}_\pm(x_\pm)$ are given by

$$\mathcal{F}_\pm(x_\pm) = k_\pm\, x_\pm^\eta \int_0^\infty dY_\pm\, Y_\pm \sin(Y_\pm x_\pm)\, g_\pm(Y_\pm), \tag{B6}$$

with the amplitudes $k_\pm$ fixed by the condition $\mathcal{F}_\pm(0)=1$ which allows one to express the nonuniversal amplitudes $C^\pm$ in terms of B_Φ and $\xi_0^\pm$. For the case $T > T_c$ the approximation for $g_+(Y_+)$ proposed by Bray [53] can be regarded to be reliable. Accordingly, for values $Y_+ \leqslant 20$ the function $g_+(Y_+)$ can be inferred from the first column in Table V of Ref. [53] whereas for $Y_+ > 20$ the asymptotic expansion by Fisher and Langer [49] is applicable, i.e.,

$$g_+(Y_+ \to \infty) = \frac{C_1}{Y_+^{2-\eta}} \left[1 + \frac{C_2}{Y_+^{(1-\alpha)/\nu}} + \frac{C_3}{Y_+^{1/\nu}} + \cdots \right], \tag{B7}$$

with coefficients C_i and the bulk critical exponents η, α, and ν. Using in Eqs. (B6) and (B7) the values $\eta = 0.041$, $\nu = 0.638$, and $\alpha = 0.086$ as quoted in Ref. [53] yields $C_1 = 0.909$, $C_2 = 3.593$, $C_3 = -4.493$ [53], and $k_+ = 0.7166$. Unfortunately, for $T < T_c$ and $D=3$ we are not aware of an accurate estimate of $g_-(Y_-)$.

(b) $D=2$. In this case the scaling functions $\mathcal{F}_\pm(x_\pm)$ are given by

$$\mathcal{F}_\pm(x_\pm) = k_\pm'\, x_\pm^\eta \int_0^\infty dY_\pm\, Y_\pm\, J_0(Y_\pm x_\pm)\, g_\pm(Y_\pm), \tag{B8}$$

where J_0 is a modified Bessel function [45]. In $D=2$ exact results for $g_\pm(Y_\pm)$ can be deduced from Ref. [52]. However,

some care is necessary regarding the definition of the scaling variable y used in Ref. [52]: whereas $y=Y_+$ for $T>T_c$, one has $y=1.959\,Y_-$ for $T<T_c$. The numerical prefactor in front of Y_- equals $(\sqrt{\Sigma_2^-}\,R_-)^{-1}$ with Σ_2^- from Table IV in Ref. [52] [see Eq. (3.7) in Ref. [52]] and with the universal amplitude ratio $R_-=\xi_0^-/\xi_{0,1}^-=1.615$ in $D=2$ [50]. For the amplitudes $k_\pm'$ in Eq. (B8) one obtains $k_+'=0.5874$ and $k_-'=0.05055$.

APPENDIX C: SMALL CURVATURE EXPANSION OF THE EXCESS ADSORPTION

In this appendix we outline how the coefficients $a_{d,D}^{\pm}$ and $b_{d,D}^{\pm}$ introduced in Eq. (3.11) can be calculated within mean-field theory, i.e., for $D=4$. Since the approaches for $T>T_c$ $(+)$ and for $T<T_c$ $(-)$ are quite similar we restrict our presentation to the case $T>T_c$.

According to Eqs. (4.3) and (4.7) for $D=4$ the universal scaling function $P_+(x_+,y_+)$ satisfies the nonlinear differential equation (in the following we drop the subscript ''+'' in order to simplify the notation)

$$P''(x,y)+\frac{d-1}{x+y}P'(x,y)-P(x,y)=P^3(x,y), \quad \text{(C1a)}$$

where the derivatives are taken with respect to the variable x. The parameter d with $1\leqslant d\leqslant 4$ can be chosen arbitrarily. Equation (C1a) is supplemented by the boundary conditions

$$P(x\to 0,y)\to\frac{\sqrt{2}}{x}, \quad P(\infty,y)=P_{+,b}=0. \quad \text{(C1b)}$$

The scaling function $G(y)\equiv G_+(y_+)$ from Eq. (3.6) then reads

$$G(y)=\int_0^\infty dx\left\{\left(\frac{x}{y}+1\right)^{d-1}P(x,y)-P_0(x)\right\} \quad \text{(C2)}$$

with $P(x,y)$ defined by Eq. (C1) and the half-space profile $P_0(x)\equiv P(x,\infty)=P_+(x_+)$ given by the first part of Eq. (2.9). Note that the singularity at $x=0$ of the first term in curly brackets in Eq. (C2) is cancelled by the second term. According to Eq. (3.11) the function $G(y)$ can be expanded as

$$G(y\to\infty)=a_d\,y^{-1}+b_d\,y^{-2}+\cdots \quad \text{(C3)}$$

with the coefficients $a_d\equiv a_{d,4}^+$ and $b_d\equiv b_{d,4}^+$ which we want to determine. To this end we expand $P(x,y)$ as

$$P(x,y\to\infty)=P_0(x)+P_1(x)\,y^{-1}+P_2(x)\,y^{-2}+\cdots. \quad \text{(C4)}$$

By inserting Eq. (C4) into Eq. (C1a) and equating terms with the same power in y one derives the familiar nonlinear differential equation for the half-space profile $P_0(x)$, i.e.,

$$P_0''-P_0=P_0^3, \quad \text{(C5a)}$$

$$P_0(x\to 0)\to\frac{\sqrt{2}}{x}, \quad P_0(\infty)=0, \quad \text{(C5b)}$$

and the two linear differential equations

$$P_1''-P_1-3P_0^2P_1=-(d-1)P_0', \quad \text{(C6a)}$$

$$P_1(0)=-\frac{\sqrt{2}}{6}(d-1), \quad P_1(\infty)=0, \quad \text{(C6b)}$$

and

$$P_2''-P_2-3P_0^2P_2=-(d-1)P_1'+3P_0P_1^2+(d-1)\,xP_0', \quad \text{(C7a)}$$

$$P_2'(0)=-\frac{\sqrt{2}}{36}(d-1)^2+\frac{\sqrt{2}}{6}(d-1), \quad P_2(\infty)=0, \quad \text{(C7b)}$$

for $P_1(x)$ and $P_2(x)$, respectively. For the boundary conditions in the second parts of the above equations compare Eqs. (4.16) and (4.7). By using

$$\left(\frac{x}{y}+1\right)^{d-1}=1+(d-1)\,x\,y^{-1}+\frac{1}{2}(d-1)(d-2)\,x^2\,y^{-2}+\cdots \quad \text{(C8)}$$

in the integrand on the RHS of Eq. (C2) in conjunction with Eq. (C4) we find for the coefficients in Eq. (C3) the expressions

$$a_d=(d-1)\int_0^\infty dx\,x\,P_0(x)+\int_0^\infty dx\,P_1(x) \quad \text{(C9)}$$

and

$$b_d=\frac{1}{2}(d-1)(d-2)\int_0^\infty dx\,x^2\,P_0(x)+(d-1)\int_0^\infty dx\,x\,P_1(x)+\int_0^\infty dx\,P_2(x), \quad \text{(C10)}$$

where $P_0(x)$, $P_1(x)$, and $P_2(x)$ are the solutions of Eqs. (C5)–(C7). While $P_0(x)$ is given by the first part of Eq. (2.9) we now turn to the calculation of $P_1(x)$ and $P_2(x)$. It is important to retain the dependence of the latter functions on d in analytical form in order to be able to carry out the consistency check of Eq. (3.13) for the present case $D=4$.

(i) Function $P_1(x)$. Both the RHS of Eq. (C6a) and the boundary condition in the first part of Eq. (C6b) depend on d via the term $(d-1)$. We note that even the full function $P_1(x)$ exhibits this simple dependence on d. The reason is that Eq. (C6a) is linear with respect to P_1 so that Eq. (C6) is solved by the ansatz

$$P_1(x)=(d-1)\,U(x), \quad \text{(C11)}$$

where $U(x)$ is independent of d and satisfies the inhomogeneous linear differential equation

$$U''-U-3P_0^2U=-P_0', \quad \text{(C12a)}$$

$$U(0)=-\frac{\sqrt{2}}{6},\quad U(\infty)=0. \tag{C12b}$$

The solution of Eq. (C12) can be given analytically (see, e.g., Ref. [43]):

$$U(x)=\frac{\cosh(x)-\sinh(x)}{6\sqrt{2}\sinh^2(x)}[2\cosh(2x)-2-3x -3x\cosh(2x)+3\sinh(2x)-3x\sinh(2x)]. \tag{C13}$$

(ii) Function $P_2(x)$. By using Eq. (C11) the differential equation (C7a) turns into

$$P_2''-P_2-3P_0^2P_2=-(d-1)^2U'+(d-1)^2 3P_0U^2 +(d-1)xP_0' \tag{C14}$$

with $U(x)$ from Eq. (C13). In this case both on the RHS of Eq. (C14) and in the boundary condition in the first part of Eq. (C7b) different dependences on d arise via the terms $(d-1)^2$ and $(d-1)$. Again it is crucial to observe that Eq. (C14) is linear with respect to P_2 so that its dependence on d takes the simple form

$$P_2(x)=(d-1)^2V(x)+(d-1)W(x) \tag{C15}$$

where $V(x)$ and $W(x)$ are independent of d and satisfy separately the inhomogeneous linear differential equations

$$V''-V-3P_0^2V=-U'+3P_0U^2, \tag{C16a}$$

$$V'(0)=-\frac{\sqrt{2}}{36},\quad V(\infty)=0, \tag{C16b}$$

and

$$W''-W-3P_0^2W=xP_0', \tag{C17a}$$

$$W'(0)=\frac{\sqrt{2}}{6},\quad W(\infty)=0. \tag{C17b}$$

Equations (C16) and (C17) can be solved numerically, which is facilitated by the fact that both $U(x)$ and $P_0(x)$ on the RHS of Eqs. (C16a) and (C17a) are known in analytical form. By inserting the resulting function $P_2(x)$ from Eq. (C15) and the function $P_1(x)$ from Eq. (C11) into Eqs. (C9) and (C10) one obtains the dependences of $a_{d,4}^{+}=a_d$ and $b_{d,4}^{+}=b_d$ on d as given by Eq. (3.13) with the curvature parameters given in the first parts of Eq. (4.21). The procedure in the case $T<T_c$ is completely analogous to that for $T>T_c$ as outlined above and yields the curvature parameters in the second parts of Eq. (4.21).

[1] W. B. Russel, D. A. Saville, and W. R. Schowalter, *Colloidal Dispersions* (Cambridge University Press, Cambridge, 1989).

[2] *Colloid Physics*, Proceedings of the *Workshop on Colloid Physics*, University of Konstanz, Germany, 1995 [Physica A **235**, 1 (1997)].

[3] T. Bieker and S. Dietrich, Physica A **252**, 85 (1998), and references therein.

[4] D. Beysens and D. Estève Phys. Rev. Lett. **54**, 2123 (1985); for a review see D. Beysens, J.-M. Petit, T. Narayanan, A. Kumar, and M. L. Broide, Ber. Bunsenges. Phys. Chem. **98**, 382 (1994).

[5] H. Löwen, Phys. Rev. Lett. **74**, 1028 (1995); Z. Phys. B **97**, 269 (1995).

[6] B. M. Law, J.-M. Petit, and D. Beysens, Phys. Rev. E **57**, 5782 (1998); J.-M. Petit, B. M. Law, and D. Beysens, J. Colloid Interface Sci. **202**, 441 (1998).

[7] K. Binder, in *Phase Transitions and Critical Phenomena*, edited by C. Domb and J. L. Lebowitz (Academic, London, 1983), Vol. 8, p. 1.

[8] H. W. Diehl, in *Phase Transitions and Critical Phenomena*, edited by C. Domb and J. L. Lebowitz (Academic, London, 1986), Vol. 10, p. 75; H. W. Diehl, Int. J. Mod. Phys. B **11**, 3503 (1997).

[9] A. J. Liu and M. E. Fisher, Phys. Rev. A **40**, 7202 (1989).

[10] J. L. Cardy, Phys. Rev. Lett. **65**, 1443 (1990).

[11] E. Eisenriegler and M. Stapper, Phys. Rev. B **50**, 10 009 (1994).

[12] H. W. Diehl and M. Smock, Phys. Rev. B **47**, 5841 (1993); **48**, 6740 (1993).

[13] M. Smock, H. W. Diehl, and D. P. Landau, Ber. Bunsenges. Phys. Chem. **98**, 486 (1994).

[14] G. Flöter and S. Dietrich, Z. Phys. B **97**, 213 (1995).

[15] D. S. P. Smith, B. M. Law, M. Smock, and D. P. Landau, Phys. Rev. E **55**, 620 (1997).

[16] J. H. Carpenter, B. M. Law, and D. S. P. Smith (unpublished).

[17] For the case of parallel plates see M. Krech and S. Dietrich, Phys. Rev. A **46**, 1886 (1992); **46**, 1922 (1992); M. Krech, *The Casimir Effect in Critical Systems* (World Scientific, Singapore, 1994); M. Krech, Phys. Rev. E **56**, 1642 (1997).

[18] Early qualitative discussions can be found in M. E. Fisher and P. G. de Gennes, C. R. Acad. Sci., Ser. B **287**, 207 (1978); P. G. de Gennes, C. R. Acad. Sci., Ser. II **292**, 701 (1981).

[19] T. W. Burkhardt and E. Eisenriegler, Phys. Rev. Lett. **74**, 3189 (1995); E. Eisenriegler and U. Ritschel, Phys. Rev. B **51**, 13 717 (1995).

[20] R. Netz, Phys. Rev. Lett. **76**, 3646 (1996).

[21] T. W. Burkhardt and E. Eisenriegler, J. Phys. A **18**, L83 (1985).

[22] S. Gnutzmann and U. Ritschel, Z. Phys. B **96**, 391 (1995).

[23] A. Hanke, F. Schlesener, E. Eisenriegler, and S. Dietrich, Phys. Rev. Lett. **81**, 1885 (1998).

[24] P. A. Buining and H. N. W. Lekkerkerker, J. Phys. Chem. **97**, 11 510 (1993); P. A. Buining, A. P. Philipse, and H. N. W. Lekkerkerker, Langmuir **10**, 2106 (1994).

[25] F. Gittes, B. Mickey, J. Nettleton, and J. Howard, J. Cell Biol. **120**, 923 (1993).

[26] S. Iijima, Nature (London) **354**, 56 (1991).

[27] *Statistical Mechanics of Membranes and Surfaces*, edited by

D. Nelson, T. Piran, and S. Weinberg (World Scientific, Singapore, 1988).

[28] U. Seifert and R. Lipowsky, in *Structure and Dynamics of Membranes*, edited by R. Lipowsky and E. Sackmann (Elsevier, Amsterdam, 1995), Vol. 1.

[29] Y. Jayalakshmi and E. W. Kaler, Phys. Rev. Lett. **78**, 1379 (1997).

[30] Such a generalized cylinder has already been introduced in the different context of the interaction between colloidal particles and flexible polymer chains in a dilute polymer solution, see E. Eisenriegler, A. Hanke, and S. Dietrich, Phys. Rev. E **54**, 1134 (1996).

[31] Any definition $\xi_{\pm}'$ different from that of $\xi_{\pm}$ as the true correlation length is related to $\xi_{\pm}$ by the universal ratio $\xi_{\pm}'/\xi_{\pm}$. This leads to a corresponding change of the scaling functions $P_{\pm}$ and of quantities obtained from them so that experimentally observable quantities remain unchanged (for more details see Appendix B and Ref. [14]).

[32] The bars on $\overline{a}_{\pm}$, $\overline{a}_{\pm}'$, $\overline{b}_{\pm}$ serve to distinguish these coefficients from the corresponding ones $a_{\pm}$, $a_{\pm}'$, $b_{\pm}$ introduced in Ref. [12] which are defined differently from Eq. (2.4).

[33] J. Zinn-Justin, *Quantum Field Theory and Critical Phenomena* (Clarendon, Oxford, 1989).

[34] The first singular contribution proportional to $\overline{b}_{\pm}$ in Eq. (2.4) can be attributed [10,11] to the leading nontrivial ''surface operator'' $\lim_{s\to 0} T_{ss}(\mathbf{r})$ with the stress tensor operator $T_{ij}(\mathbf{r})$ whose scaling dimension is equal to the spatial dimension D.

[35] R. Z. Bariev, Theor. Math. Phys. **77**, 1090 (1988).

[36] The curves for $P_{-}(x_{-})$ for $D=4$ shown in Fig. 2 of Ref. [13] and in Fig. 1(b) of Ref. [14], which do not comply with this statement, are not correct.

[37] See, e.g., the article of F. David in Ref. [27].

[38] We briefly outline the argument: Since the curvature contributions must depend on how the surface is embedded in the space $\mathbb{R}^D$ they must be derivable from the local extrinsic curvature tensor $\mathbf{K}_{ij}=K_{ij}\,\mathbf{n}$ where $\mathbf{n}$ is the local unit vector normal to the surface (we only consider orientable surfaces). The principal local radii of curvature R_i are the inverse of the $D-1$ eigenvalues of the matrix (K_{ij}). Therefore K_m, K_m^2, and K_G as defined in Eq. (2.17) are the only independent scalar quantities to first and second order in $1/R_i$ which can be deduced from K_{ij} and which are invariant under permutations of the indices $i=1,\ \ldots\ ,D-1$.

[39] The leading regular term captured by the ellipses in Eq. (2.23) which is analytic in $1/R$ is proportional to $t/R\sim\xi_{\pm}^{-1/\nu}/R$. Since all terms in curly brackets depend only on the dimensionless variables $x_{\pm}$ and $y_{\pm}$ this regular term must scale with $x_{\pm}^{1+1/\nu}$ where the exponent is larger than two if $D>2$.

[40] The dashed line in Fig. 3 is known rather accurately by means of the ε expansions of $\beta(D)$ and $\nu(D)$ in conjunction with the corresponding exact values in $D=2$ [33].

[41] In a lattice model such a ''cylinder'' with microscopically small radius R can be realized by a single line of lattice sites where the orientation of the spins is fixed.

[42] It is instructive to interpret Eq. (4.3) as an equation of motion of a particle at ''position'' m and ''time'' s subjected to the ''potential energy'' $-\tau m^2/2-m^4/4$ [7,8]. In general the differential equation cannot be solved analytically due to the time-dependent friction term. One seeks solutions $m(s)$ which come at rest on the top m_b of the potential hill at time $s\to\infty$. This problem can be solved numerically, e.g., by means of a ''shooting method'' as a trial and error approach.

[43] C. M. Bender and S. A. Orszag, *Advanced Mathematical Methods for Scientists and Engineers* (McGraw-Hill, New York, 1978).

[44] Compare, e.g., P. J. Upton, J. O. Indekeu, and J. M. Yeomans, Phys. Rev. B **40**, 666 (1989), and Ref. [7].

[45] (a) M. Abramowitz and I. A. Stegun, *Handbook of Mathematical Functions* (Dover, New York, 1972); (b) I. S. Gradshteyn and I. M. Ryzhik, *Table of Integrals, Series, and Products* (Academic, London, 1965).

[46] The curvature parameters for a convex surface as considered here should, of course, be the same as for a concave surface. In the present mean-field case this does indeed hold. This can be confirmed by using the methods outlined in Appendix C.

[47] T. Gil and J. H. Ipsen, Phys. Rev. E **55**, 1713 (1997); T. Gil, M. C. Sabra, J. H. Ipsen, and O. G. Mouritsen, Biophys. J. **73**, 1728 (1997).

[48] H.-G. Döbereiner, E. Evans, M. Kraus, U. Seifert, and M. Wortis, Phys. Rev. E **55**, 4458 (1997).

[49] M. E. Fisher and J. S. Langer, Phys. Rev. Lett. **20**, 665 (1968).

[50] H. B. Tarko and M. E. Fisher, Phys. Rev. Lett. **31**, 926 (1973).

[51] H. B. Tarko and M. E. Fisher, Phys. Rev. B **11**, 1217 (1975).

[52] C. A. Tracy and B. M. McCoy, Phys. Rev. B **12**, 368 (1975).

[53] A. J. Bray, Phys. Rev. B **14**, 1248 (1976).

[54] A. J. Liu and M. E. Fisher, Physica A **156**, 35 (1989).